Pergamon

Int. J. Solids Structures Vol. 33, No. 20–22, pp. 2993–3017, 1996
Copyright © 1996 Elsevier Science Ltd
Printed in Great Britain. All rights reserved
0020-7683/96 $15.00 + .00

0020-7683(95)00251-0

ON A SYSTEMATIC DEVELOPMENT OF TRILINEAR THREE-DIMENSIONAL SOLID ELEMENTS BASED ON SIMO'S ENHANCED STRAIN FORMULATION

C. FREISCHLÄGER and K. SCHWEIZERHOF
Institute for Theoretical Mechanics and Institute for Mechanics, University(TH) Karlsruhe, Germany

Abstract—A systematic development of eight-node trilinear three-dimensional solid elements based on Simo's theoretical framework for the enhanced assumed strain formulation is presented for linear elasticity. The starting point is a regular brick followed by parallelepipeds and then arbitrarily distorted elements. The advantages and deficits of various enhanced strain formulations are extensively discussed using the regular brick. For arbitrarily distorted elements a simple modification of the element-stiffness matrix is proposed to achieve a more reliable and very efficient element. On some numerical examples the advantages and limits of the family of enhanced strain elements and the improved elements are discussed. Copyright © 1996 Elsevier Science Ltd.

1. INTRODUCTION

Three-dimensional solid elements with low order interpolation functions, which are free of locking effects and which can be applied also to nonlinear problems in a fashion similar to standard displacement models, have been in the focus of active research in recent years. The fundamental and comprehensive paper of Simo and Rifai (1990), in which the so-called "enhanced assumed strain method" was proposed, opened a new way to handle large three-dimensional problems efficiently. First developed for geometrically linear and small-strain plasticity analysis, this powerful method was extended by Simo and Armero (1992) and Simo *et al.* (1993) to problems with strong geometrical and material nonlinearities.

The aim of the non-constant enhanced strains is to remove the undesirable stiffening of the standard eight-node displacement-based solid element in bending dominated problems as well as in modeling nearly incompressible material; the well-known shear and incompressibility-locking. These two locking phenomena are responsible for the low quality of the standard displacement element.

The EAS-method can be interpreted as a $\bar{\mathbf{B}}$-method. The $\bar{\mathbf{B}}$-matrix is obtained after the static condensation of the enhanced strain parameters on the element level. Contrary to many $\bar{\mathbf{B}}$-formulations involving some heuristics, as described for example by Belytschko and Bindeman (1993), Simo's method provides a variational consistent way for the derivation of the $\bar{\mathbf{B}}$-matrix. At this point it has to be mentioned that the EAS elements contain important ingredients from all the other popular methods attempting to solve the above mentioned problem, the so-called $\bar{\mathbf{B}}$-elements suggested by Hughes and Malkus (1978), the four-node plane stress element of Pian–Sumihara (1984) and in particular the hourglass controlled elements suggested by Belytschko *et al.* (1984); Belytschko and Bindeman (1991, 1993); Flanagan and Belytschko (1981) and Liu *et al.*, (1985). The relation of the EAS-elements to the so-called Hellinger–Reissner elements with independent interpolation of stresses has been pointed out by Andelfinger and Ramm (1993). The latter authors have also given a first discussion on one of the following open questions when working with the enhanced assumed strain method in three dimensions: (a) which and how many enhanced strain terms are needed to remove locking and (b) how can the time-consuming static condensation procedure be avoided, in particular for the solution of nonlinear problems?

For the second question a satisfactory solution has still to be found in opposition to the Hellinger–Reissner elements, for which the static condensation of the stress-parameters can be avoided with a simple approximation, the so-called admissible matrix formulation developed by Sze (1992).

The primary aim of the current study is to further elaborate on the development of enhanced strain terms in order to gain more insight into the effect of the various terms and also to limit the number of additional terms for efficiency reasons. The secondary aim is the development of an efficient EAS-element without static condensation and thereby using the possibility of an exact symbolic integration. This idea is based on splitting the element-stiffness matrix into a matrix ensuring convergence and a so-called stabilization matrix. The influence of the enhanced strains is found to be only represented by this stabilization matrix. The formulation of the matrix which ensures convergence was first given by Belytschko and Bindeman (1993) whilst investigating the problem of accurate representation of constant strain states for three-dimensional distorted meshes.

2. BASIC CONSIDERATIONS

In order to provide a basis for the development of the new three-dimensional solid elements, a brief introduction into the basic equations for enhanced assumed strain (EAS) elements following the ideas of Simo and Rifai (1990) is given. According to their suggestions, the development of a new eight-node three-dimensional element is based on the Hu–Washizu functional for linear elastic material with independent stresses $\boldsymbol{\sigma}$, independent strains $\boldsymbol{\varepsilon}$, displacements $\mathbf{u}$ and the symmetric part of the displacement gradient $\boldsymbol{\varepsilon}_u$:

$$\Pi_{HW} = \frac{1}{2}\int_{V_e} \boldsymbol{\varepsilon}^T \mathbf{C}\boldsymbol{\varepsilon}\, dv_e + \int_{V_e} \boldsymbol{\sigma}^T(\boldsymbol{\varepsilon}_u - \boldsymbol{\varepsilon})\, dv_e - \Pi_{ext}(\mathbf{u}). \tag{1}$$

Π_{ext} is the functional of body-forces and surface tractions. V_e is the volume enclosed by an element. $\mathbf{C}$ is the elasticity or stress–strain matrix, which has the following form for isotropic material:

$$\mathbf{C}_{iso} = \begin{bmatrix} E1 & E2 & E2 & 0 & 0 & 0 \\ E2 & E1 & E2 & 0 & 0 & 0 \\ E2 & E2 & E1 & 0 & 0 & 0 \\ 0 & 0 & 0 & G & 0 & 0 \\ 0 & 0 & 0 & 0 & G & 0 \\ 0 & 0 & 0 & 0 & 0 & G \end{bmatrix} \quad \text{with:} \quad \begin{aligned} E1 &= \frac{E(1-\nu)}{(1+\nu)(1-2\nu)} \\ E2 &= \frac{Eu}{(1+\nu)(1-2\nu)} \\ G &= \frac{E}{2(1+\nu)} \end{aligned} \tag{2}$$

The displacements $\mathbf{u} = (u, v, w)^T$ and the components of the position vector $\mathbf{x} = (x, y, z)^T$ in the element are represented by the nodal displacements u^i or nodal coordinates x^i, respectively, and standard trilinear shape functions $n_i = \frac{1}{8}(1+r_i r)(1-s_i s)(1+t_i t)$ $(i = 1, \ldots, 8)$, see e.g. Fig. 1. Following Belytschko *et al.* (1984) the shape-functions can also be written as a linear combination of linear polynomials in Cartesian coordinates x, y, z and four hour-glass functions g_i (see also Simo *et al.*, 1993):

$$\mathbf{u} = \begin{bmatrix} u \\ v \\ w \end{bmatrix} = \sum_{i=1}^{8} \begin{bmatrix} n_i u^i \\ n_i v^i \\ n_i w^i \end{bmatrix} = \begin{bmatrix} \mathbf{n}^T & \mathbf{0}^T & \mathbf{0}^T \\ \mathbf{0}^T & \mathbf{n}^T & \mathbf{0}^T \\ \mathbf{0}^T & \mathbf{0}^T & \mathbf{n}^T \end{bmatrix} \mathbf{u}_e,$$

$$\mathbf{x} = \begin{bmatrix} x \\ y \\ z \end{bmatrix} = \sum_{i=1}^{8} n^i \begin{bmatrix} n_i x^i \\ n_i y^i \\ n_i z^i \end{bmatrix} = \begin{bmatrix} \mathbf{n}^T & \mathbf{0}^T & \mathbf{0}^T \\ \mathbf{0}^T & \mathbf{n}^T & \mathbf{0}^T \\ \mathbf{0}^T & \mathbf{0}^T & \mathbf{n}^T \end{bmatrix} \mathbf{x}_e, \tag{3}$$

with the vector of shape functions

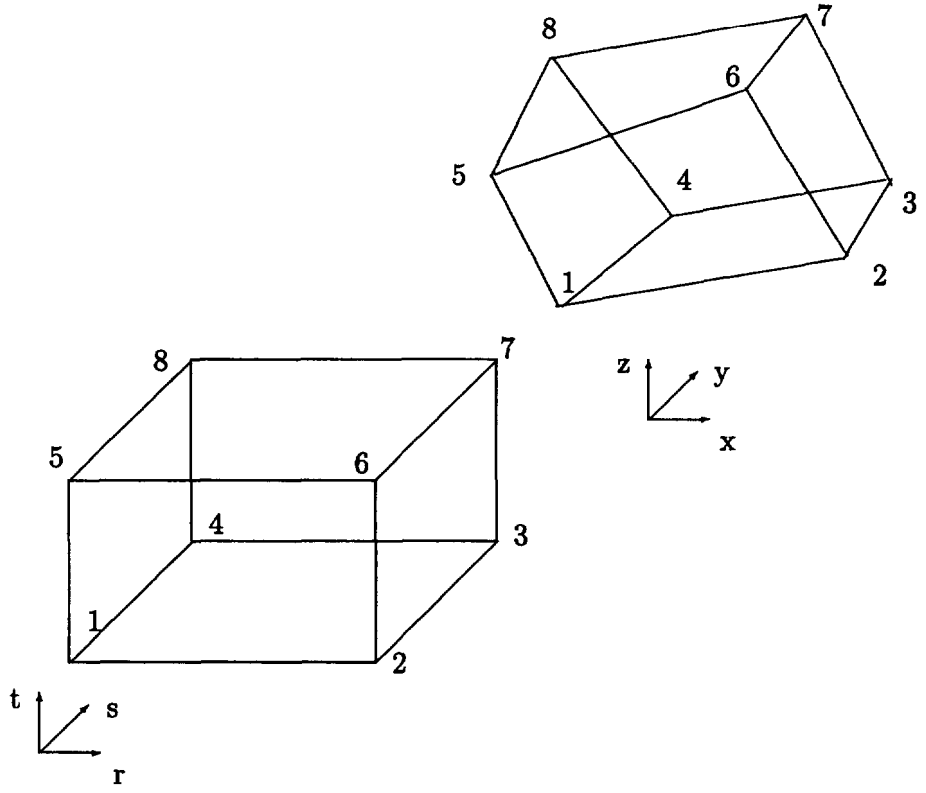

Fig. 1. Element in reference and physical coordinate system.

$$\mathbf{n} = \mathbf{n}_0 + x\mathbf{b}_x + y\mathbf{b}_y + z\mathbf{b}_z + g_1\gamma_1 + g_2\gamma_2 + g_3\gamma_3 + g_4\gamma_4, \tag{4}$$

and the so-called γ-projection vectors ($\mathbf{x}$, $\mathbf{y}$, $\mathbf{z}$ are the nodal coordinate vectors);

$$\gamma_i = \mathbf{h}_i - (\mathbf{h}_i^{\mathrm{T}}\mathbf{x})\mathbf{b}_x - (\mathbf{h}_i^{\mathrm{T}}\mathbf{y})\mathbf{b}_y - (\mathbf{h}_i^{\mathrm{T}}\mathbf{z})\mathbf{b}_z \quad (i = 1 \ldots, 4), \quad (\mathbf{b}_x, \mathbf{b}_y, \mathbf{b}_z) = \left(\frac{\partial \mathbf{n}}{\partial x}, \frac{\partial \mathbf{n}}{\partial y}, \frac{\partial \mathbf{n}}{\partial z}\right)_{(0)},$$

$$\mathbf{n}_0 = \mathbf{e} - (\mathbf{e}^{\mathrm{T}}\mathbf{x})\mathbf{b}_x - (\mathbf{e}^{\mathrm{T}}\mathbf{y})\mathbf{b}_y - (\mathbf{e}^{\mathrm{T}}\mathbf{z})\mathbf{b}_z, \quad \mathbf{e} = \tfrac{1}{8}(1,1,1,1,1,1,1,1)^{\mathrm{T}}$$

$$g_1 = rs, \quad g_2 = rt, \quad g_3 = st, \quad g_4 = rst. \tag{5}$$

If the Jacobian-matrix $\mathbf{J} = \partial(x, y, z)/\partial(r, s, t)$ is constant within the element—the element has the shape of a brick or a parallelepiped—the γ-vectors reduce to the simple so-called hour-glass vectors $\mathbf{h}_1 \ldots, \mathbf{h}_4$:

$$\mathbf{n} = \mathbf{n}_0 + x\mathbf{b}_x + y\mathbf{b}_y + z\mathbf{b}_z + g_1\mathbf{h}_1 + g_2\mathbf{h}_2 + g_3\mathbf{h}_3 + g_4\mathbf{h}_4 \tag{6}$$

and

$$[\mathbf{h}_1, \mathbf{h}_2, \mathbf{h}_3, \mathbf{h}_4] = \tfrac{1}{8}\begin{bmatrix} +1 & +1 & +1 & -1 \\ -1 & -1 & +1 & +1 \\ +1 & -1 & -1 & -1 \\ -1 & +1 & -1 & +1 \\ +1 & -1 & -1 & +1 \\ -1 & +1 & -1 & -1 \\ +1 & +1 & +1 & +1 \\ -1 & -1 & +1 & -1 \end{bmatrix}. \tag{7}$$

The strains are given as:

$$\boldsymbol{\varepsilon}_u = \begin{bmatrix} \varepsilon_x \\ \varepsilon_y \\ \varepsilon_z \\ 2\varepsilon_{xy} \\ 2\varepsilon_{xz} \\ 2\varepsilon_{yz} \end{bmatrix} = \begin{bmatrix} \frac{\partial \mathbf{n}^T}{\partial x} & \mathbf{0}^T & \mathbf{0}^T \\ \mathbf{0}^T & \frac{\partial \mathbf{n}^T}{\partial y} & \mathbf{0}^T \\ \mathbf{0}^T & \mathbf{0}^T & \frac{\partial \mathbf{n}^T}{\partial z} \\ \frac{\partial \mathbf{n}^T}{\partial y} & \frac{\partial \mathbf{n}^T}{\partial x} & \mathbf{0}^T \\ \frac{\partial \mathbf{n}^T}{\partial z} & \mathbf{0}^T & \frac{\partial \mathbf{n}^T}{\partial x} \\ \mathbf{0}^T & \frac{\partial \mathbf{n}^T}{\partial z} & \frac{\partial \mathbf{n}^T}{\partial y} \end{bmatrix} \begin{bmatrix} \mathbf{u} \\ \mathbf{v} \\ \mathbf{w} \end{bmatrix} = \mathbf{B}\mathbf{u}_e. \tag{8}$$

Through insertion of eqn (4) into eqn (8) the conventional strain–displacement matrix $\mathbf{B}$, which consists of a constant part $\mathbf{B}_c$ and a position dependent part $\mathbf{B}_h$, can be written as:

$$\boldsymbol{\varepsilon}_u = \mathbf{B}\mathbf{u}_e = (\mathbf{B}_c + \mathbf{B}_h) \begin{bmatrix} \mathbf{u} \\ \mathbf{v} \\ \mathbf{w} \end{bmatrix},$$

with

$$\mathbf{B} = \mathbf{B}_c + \mathbf{B}_h = \begin{bmatrix} \mathbf{b}_x^T & \mathbf{0}^T & \mathbf{0}^T \\ \mathbf{0}^T & \mathbf{b}_y^T & \mathbf{0}^T \\ \mathbf{0}^T & \mathbf{0}^T & \mathbf{b}_z^T \\ \mathbf{b}_y^T & \mathbf{b}_x^T & \mathbf{0}^T \\ \mathbf{b}_z^T & \mathbf{0}^T & \mathbf{b}_x^T \\ \mathbf{0}^T & \mathbf{b}_z^T & \mathbf{b}_y^T \end{bmatrix} + \begin{bmatrix} \frac{\partial g_k}{\partial x}\boldsymbol{\gamma}_k^T & \mathbf{0}^T & \mathbf{0}^T \\ \mathbf{0}^T & \frac{\partial g_k}{\partial y}\boldsymbol{\gamma}_k^T & \mathbf{0}^T \\ \mathbf{0}^T & \mathbf{0}^T & \frac{\partial g_k}{\partial z}\boldsymbol{\gamma}_k^T \\ \frac{\partial g_k}{\partial y}\boldsymbol{\gamma}_k^T & \frac{\partial g_k}{\partial x}\boldsymbol{\gamma}_k^T & \mathbf{0}^T \\ \frac{\partial g_k}{\partial z}\boldsymbol{\gamma}_k^T & \mathbf{0}^T & \frac{\partial g_k}{\partial x}\boldsymbol{\gamma}_k^T \\ \mathbf{0}^T & \frac{\partial g_k}{\partial z}\boldsymbol{\gamma}_k^T & \frac{\partial g_k}{\partial y}\boldsymbol{\gamma}_k^T \end{bmatrix} \quad k = 1, \ldots, 4. \tag{9}$$

Following Simo and Rifai (1990) the strains $\boldsymbol{\varepsilon}$ can be assumed to consist of the displacement derivatives $\mathbf{B}\mathbf{u}_e$, which are the strains of the pure displacement element and enhanced incompatible strains $\boldsymbol{\varepsilon}^{(i)}$. The enhanced strains $\boldsymbol{\varepsilon}_k^{(i)}$ $(k = 1, \ldots, 6)$ are defined in the element by local element parameters (included in the vector $\boldsymbol{\phi}_e$) and interpolation functions (included in the matrix $\mathbf{G}$):

$$\boldsymbol{\varepsilon} = \mathbf{B}\mathbf{u}_e + \boldsymbol{\varepsilon}^{(i)} = \mathbf{B}\mathbf{u}_e + \mathbf{G}\boldsymbol{\phi}_e \quad \boldsymbol{\phi}_e \in R^{\text{eas}}. \tag{10}$$

The choice of the element parameters and the interpolation functions will be a main aspect of the following discussion. The functional shown in eqn (1) is rather simplified with this specific choice of an enhanced strain field:

$$\Pi_{HW} = \frac{1}{2}\int_{V_e} \boldsymbol{\varepsilon}^T \mathbf{C}\boldsymbol{\varepsilon}\, dv_e + \int_{V_e} \boldsymbol{\sigma}^T \boldsymbol{\varepsilon}^{(i)}\, dv_e - \Pi_{ext}(\mathbf{u}). \tag{11}$$

To get a two-field functional, orthogonality between stresses and enhanced strains is required:

$$\int_{V_e} \boldsymbol{\sigma}^T \boldsymbol{\varepsilon}^{(i)}\, dv_e = 0. \tag{12}$$

This requirement must also be fulfilled for any constant stress state (see Simo and Rifai, 1990), thus:

$$\int_{V_e} \boldsymbol{\varepsilon}^{(i)}\, dv_e = 0 \quad \Leftrightarrow \quad \int_{V_e} \mathbf{G}\, dv_e = 0. \tag{13}$$

Following the suggestion of Simo and Rifai (1990) to set up the matrix $\mathbf{G}$ in the reference system in local element coordinates and then transform it with the constant transformation matrix $\mathbf{T}_0$ into the global Cartesian coordinate system (see also Andelfinger and Ramm, 1993), we obtain:

$$\mathbf{G} = \frac{j_0}{\det} \mathbf{T}_0 \mathbf{G}_\xi. \tag{14}$$

Thereby the factor $j_0/\det$, i.e. the ratio of the determinant of the Jacobian matrix at the element-origin $\boldsymbol{\xi} = (0,0,0)^T$ and the position $\boldsymbol{\xi} = (r,s,t)^T$, guarantees fulfilment of the orthogonality requirement (13) for any element shape. As a consequence of the orthogonality condition the three-field functional (1) is reduced to a two-field functional containing only independent displacements and enhanced strains:

$$\Pi = \tfrac{1}{2}\mathbf{u}_e^T \int_{V_e} \mathbf{B}^T\mathbf{C}(\mathbf{B}\mathbf{u}_e + \mathbf{G}\boldsymbol{\phi}_e)\, dv_e + \tfrac{1}{2}\boldsymbol{\phi}_e^T \int_{V_e} \mathbf{G}^T\mathbf{C}(\mathbf{B}\mathbf{u}_e + \mathbf{G}\boldsymbol{\phi}_e)\, dv_e. \tag{15}$$

Through independent variation of nodal displacements $\mathbf{u}_e$ and EAS-parameters $\boldsymbol{\phi}_e$, a system of equations on the element level is obtained:

$$\delta\Pi = 0 \quad \forall \delta\mathbf{u}_e, \delta\boldsymbol{\phi}_e \Rightarrow \begin{bmatrix} \int_{V_e} \mathbf{B}^T\mathbf{C}\mathbf{B}\, dv_e & \int_{V_e} \mathbf{B}^T\mathbf{C}\mathbf{G}\, dv_e \\ \int_{V_e} \mathbf{G}^T\mathbf{C}\mathbf{B}\, dv_e & \int_{V_e} \mathbf{G}^T\mathbf{C}\mathbf{G}\, dv_e \end{bmatrix} \begin{bmatrix} \mathbf{u}_e \\ \boldsymbol{\phi}_e \end{bmatrix} = \begin{bmatrix} \mathbf{f}_{ext} \\ \mathbf{0} \end{bmatrix}. \tag{16}$$

Taking into account that $\mathbf{B}$ is split into a constant part and a position-dependent part $\mathbf{B} = \mathbf{B}_c + \mathbf{B}_h$ and $\int_{V_e} \mathbf{G}\, dv_e = 0$, we get:

$$\begin{bmatrix} \int_{V_e} \mathbf{B}^T\mathbf{C}\mathbf{B}\, dv_e & \int_{V_e} \mathbf{B}_h^T\mathbf{C}\mathbf{G}\, dv_e \\ \int_{V_e} \mathbf{G}^T\mathbf{C}\mathbf{B}_h\, dv_e & \int_{V_e} \mathbf{G}^T\mathbf{C}\mathbf{G}\, dv_e \end{bmatrix} \begin{bmatrix} \mathbf{u}_e \\ \boldsymbol{\phi}_e \end{bmatrix} = \begin{bmatrix} \mathbf{f}_{ext} \\ \mathbf{0} \end{bmatrix}. \tag{17}$$

The system of eqn (17) can be rewritten considering the following definitions:

$$\mathbf{K} = \int_{V_e} \mathbf{B}^T \mathbf{C} \mathbf{B} \, dv_e \qquad \mathbf{K} \in R^{24 \times 24},$$

$$\mathbf{H} = \int_{V_e} \mathbf{G}^T \mathbf{C} \mathbf{G} \, dv_e \qquad \mathbf{H} \in R^{eas \times eas},$$

$$\mathbf{L} = \int_{V_e} \mathbf{G}^T \mathbf{C} \mathbf{B}_h \, dv_e \qquad \mathbf{L} \in R^{eas \times 24}, \tag{18}$$

in a more compact form:

$$\mathbf{K}\mathbf{u}_e + \mathbf{L}^T \boldsymbol{\phi}_e = \mathbf{f}_{ext} \tag{19}$$

$$\mathbf{L}\mathbf{u}_e + \mathbf{H}\boldsymbol{\phi}_e = 0 \quad \Rightarrow \boldsymbol{\phi}_e = -\mathbf{H}^{-1}\mathbf{L}\mathbf{u}_e. \tag{20}$$

Because the EAS-parameters $\boldsymbol{\phi}_e$ are not connected to any external nodal loads and the incompatible strains are discontinuous over element boundaries, $\boldsymbol{\phi}_e$ can be eliminated by inversion of the positive definite matrix $\mathbf{H}$. Insertion of eqn (20) into eqn (19) results in an element-stiffness matrix $\mathbf{K}_e$:

$$\begin{aligned} \mathbf{K}_e &= \mathbf{K} - \mathbf{L}^T \mathbf{H}^{-1} \mathbf{L} \\ &= \int_{V_e} (\mathbf{B} - \mathbf{G}\mathbf{H}^{-1}\mathbf{L})^T \mathbf{C} (\mathbf{B} - \mathbf{G}\mathbf{H}^{-1}\mathbf{L}) \, dv_e \\ &= \int_{V_e} \bar{\mathbf{B}}^T \mathbf{C} \bar{\mathbf{B}} \, dv_e, \end{aligned} \tag{21}$$

with

$$\bar{\mathbf{B}} = \mathbf{B}_c + \mathbf{B}_h - \mathbf{G}\mathbf{H}^{-1}\mathbf{L} = \mathbf{B}_c + \bar{\mathbf{B}}_h. \tag{22}$$

Thus the differences between various assumptions for the enhanced strains become visible in the $\mathbf{G}$, $\mathbf{H}$, $\mathbf{L}$ and $\bar{\mathbf{B}}_h$ matrices, which is the topic of the following sections. As the computation of $\bar{\mathbf{B}}_h$ requires the inversion of $\mathbf{H}$ it is of particular interest to reduce the computational effort as much as possible.

3. $\bar{\mathbf{B}}$-MATRICES FOR ENHANCED ASSUMED STRAIN ELEMENTS

Enhanced strain terms are introduced to eliminate the deficiencies of the standard trilinear hexahedral displacement element. This can be most clearly described and discussed looking at a rectangular brick. For this regular brick the corresponding $\bar{\mathbf{B}}_h$ matrices have a special form, which can be explicitly computed without inverting the $\mathbf{H}$ matrix numerically. These explicitly defined matrices also allow the symbolic computation of the eigenvalues of the element, thus the advantage and deficiencies of different enhancements can be shown. Based on the formulations for a rectangular brick element the $\bar{\mathbf{B}}_h$ matrices for a parallelepiped can be also developed explicitly, as the inversion of $\mathbf{H}$ can be performed symbolically. For hexahedral elements of arbitrary form the $\mathbf{H}$ matrix can no longer be explicitly inverted as the Jacobian matrix is no longer constant within an element and some approximations are necessary to achieve the goal of a reliable (i.e. locking-free, non-kinematic) and efficient element. Within the following subsections the above-mentioned aspects are presented and discussed in detail.

3.1. *Regular bricks*

The most simple three-dimensional isoparametric eight-node element is a regular brick with sides parallel to the global Cartesian coordinate axes. This special configuration has the advantage compared to an element of arbitrary shape that it allows a simple mechanical interpretation of the strain field and the direct computation of the eigenvalues of the stiffness matrix. The derivatives with respect to Cartesian coordinates x, y, z are proportional to the derivatives with respect to local element coordinates r, s, t, because the Jacobian matrix is constant and diagonal:

$$\begin{bmatrix} \frac{\partial}{\partial x} \\ \frac{\partial}{\partial y} \\ \frac{\partial}{\partial z} \end{bmatrix} = \begin{bmatrix} \frac{2}{a} & 0 & 0 \\ 0 & \frac{2}{b} & 0 \\ 0 & 0 & \frac{2}{c} \end{bmatrix} \begin{bmatrix} \frac{\partial}{\partial r} \\ \frac{\partial}{\partial s} \\ \frac{\partial}{\partial t} \end{bmatrix} \quad (a, b, c: \text{side-lengths of the brick in } x, y\text{- and } z\text{-direction}). \tag{23}$$

The non-constant coordinate dependent part $\mathbf{B}_h$ of the strain–displacement matrix possesses a very simple form, which gives a clear picture of the locking reasons of the pure displacement formulation:

$$\mathbf{B}_h = \begin{bmatrix} \frac{2}{a}(s\mathbf{h}_1^T + t\mathbf{h}_2^T + st\mathbf{h}_4^T) & \mathbf{0}^T & \mathbf{0}^T \\ \mathbf{0}^T & \frac{2}{b}(r\mathbf{h}_1^T + t\mathbf{h}_3^T + rt\mathbf{h}_4^T) & \mathbf{0}^T \\ \mathbf{0}^T & \mathbf{0}^T & \frac{2}{c}(r\mathbf{h}_2^T + s\mathbf{h}_3^T + rs\mathbf{h}_4^T) \\ \frac{2}{b}(r\mathbf{h}_1^T + t\mathbf{h}_3^T + rt\mathbf{h}_4^T) & \frac{2}{a}(s\mathbf{h}_1^T + t\mathbf{h}_2^T + st\mathbf{h}_4^T) & \mathbf{0}^T \\ \frac{2}{c}(r\mathbf{h}_2^T + s\mathbf{h}_3^T + rs\mathbf{h}_4^T) & \mathbf{0}^T & \frac{2}{a}(s\mathbf{h}_1^T + t\mathbf{h}_2^T + st\mathbf{h}_4^T) \\ \mathbf{0}^T & \frac{2}{c}(r\mathbf{h}_2^T + s\mathbf{h}_3^T + rs\mathbf{h}_4^T) & \frac{2}{b}(r\mathbf{h}_1^T + t\mathbf{h}_3^T + rt\mathbf{h}_4^T) \end{bmatrix} \tag{24}$$

$\mathbf{h}_1, \ldots, \mathbf{h}_4$ are the hour-glass vectors, see eqn (7).

Shear locking. It is directly visible that the linear normal strains, which are activated in bending, are coupled with linear shear strains, for example ε_x and γ_{xy} in the terms $s(\mathbf{h}_1^T\mathbf{u})$ and $r(\mathbf{h}_1^T\mathbf{u})$. A pure bending state therefore cannot be represented exactly and, in addition, for thin elements shear-locking occurs, because the shear-stiffness is very large compared to the bending-stiffness. This behavior can be explained looking at the internal energy in the case of pure bending in x-direction about the z-axis. For pure bending the nodal displacements $\mathbf{u} \propto \mathbf{h}_1$, $\mathbf{v} = 0$, $\mathbf{w} = 0$ cause the following strain-field:

$$\varepsilon = \left(\frac{2}{a}(\mathbf{h}_1^T\mathbf{u})s, \quad 0, \quad 0, \quad \frac{2}{b}(\mathbf{h}_1^T\mathbf{u})r, \quad 0, \quad 0\right)^T. \tag{25}$$

Thus the internal energy becomes assuming a Poisson ratio of $\nu = 0$ for simplicity:

$$\Pi_i = \frac{1}{2}\int_{V_e} \boldsymbol{\varepsilon}_x \cdot \boldsymbol{\sigma}_x \, dv_e + \frac{1}{4}\int_{V_e} \boldsymbol{\gamma}_{xy} \cdot \boldsymbol{\sigma}_{xy} \, dv_e =: \Pi_n + \Pi_s,$$

with

$$\Pi_n = \frac{1}{2}\int_{V_e} E\varepsilon_x^2 \, dv_e = \frac{2}{3} E \frac{bc}{a} (\mathbf{h}_1^T \mathbf{u})^2,$$

$$\Pi_s = \frac{1}{4}\int_{V_e} G\gamma_{xy}^2 \, dv_e = \frac{1}{3} G \frac{ac}{b} (\mathbf{h}_1^T \mathbf{u})^2 \Rightarrow \frac{\Pi_s}{\Pi_n} = \frac{Ga^2}{2Eb^2} \xrightarrow{b \ll a} \infty. \tag{26}$$

With the increasing ratio of the element length a to width b, the internal energy $\Pi_i = \frac{1}{2}\mathbf{u}_e^T \mathbf{K}_e \mathbf{u}_e$, and thus the "bending–stiffness" increases without any limit, solely because the parasitic shear strain γ_{xy} is increasing.

The eigenvalues e_j of the bending-modes (the modes of the stiffness-matrix which would represent bending without the parasitic shear strains) approach the following values assuming a Poisson ratio of $\nu = 0$:

(i) For bending in x-direction about the z-axis,

$$e_1 = \frac{1}{6ab}(Ecb^2 + Gca^2) \xrightarrow{a \gg b,c} G\frac{c}{6b} a \to \infty;$$

(ii) For bending in x-direction about the y-axis,

$$e_2 = \frac{1}{6ac}(Ebc^2 + Gba^2) \xrightarrow{a \gg b,c} G\frac{b}{6c} a \to \infty;$$

(iii) For bending in y-direction about the z-axis,

$$e_3 = \frac{1}{6ab}(Eca^2 + Gcb^2) \xrightarrow{b \gg a,c} G\frac{c}{6a} b \to \infty;$$

(iv) For bending in y-direction about the x-axis,

$$e_4 = \frac{1}{6cb}(Eac^2 + Gab^2) \xrightarrow{b \gg a,c} G\frac{a}{6c} b \to \infty;$$

(v) For bending in z-direction about the x-axis,

$$e_5 = \frac{1}{6ac}(Eba^2 + Gbc^2) \xrightarrow{c \gg b,a} G\frac{b}{6a} c \to \infty;$$

(vi) For bending in z-direction about the y-axis,

$$e_6 = \frac{1}{6cb}(Eab^2 + Gac^2) \xrightarrow{c \gg b,a} G\frac{a}{6b} c \to \infty.$$

The coupling of linear normal and shear strains causes nonphysical bending–stiffness terms, e.g. (i) and (ii) represent bending about the z- and y-axis in x-direction and their stiffness terms are for $a \gg c, b$ proportional to a. However, the bending–stiffness of the continuum becomes infinitely small with increasing length of the brick!

Incompressibility locking. The stiffening in the case of incompressibility, the so-called incompressibility-locking, is caused by missing terms in the normal strains. The constraint of an incompressible material, $\mathrm{tr}(\boldsymbol{\varepsilon}) = \varepsilon_x + \varepsilon_y + \varepsilon_z = 0$, cannot be fulfilled by the normal strains of the pure displacement element. The effect of this deficiency on the deformation behavior of an element can be again explained using the internal energy. The internal energy Π_i of an element consists of a deviatoric and a dilatational term and as it is defined by $\Pi_i = \frac{1}{2}\mathbf{u}_e^T \mathbf{K}_e \mathbf{u}_e$, the relative contribution of deviatoric and dilatational deformation to the element stiffness can be also shown:

$$\begin{aligned}\Pi_i &= \Pi_{\mathrm{dev}} + \Pi_{\mathrm{dil}} \\ &= 2G\int_{V_e} \boldsymbol{\varepsilon}_{\mathrm{dev}} : \boldsymbol{\varepsilon}_{\mathrm{dev}}\, \mathrm{d}v_e + 3K\int_{V_e} \boldsymbol{\varepsilon}_{\mathrm{dil}} : \boldsymbol{\varepsilon}_{\mathrm{dil}}\, \mathrm{d}v_e \\ &= 2G\int_{V_e} \boldsymbol{\varepsilon}_{\mathrm{dev}} : \boldsymbol{\varepsilon}_{\mathrm{dev}}\, \mathrm{d}v_e + K\int_{V_e} \mathrm{tr}(\boldsymbol{\varepsilon})^2\, \mathrm{d}v_e \quad \text{with} \quad K = \frac{2}{3}\frac{(1+\nu)}{(1-2\nu)}G. \end{aligned} \tag{27}$$

The bulk modulus K becomes very large for $\nu \to \frac{1}{2}$. If $\mathrm{tr}(\boldsymbol{\varepsilon})$ is not vanishing, the stiffness of one element or a group of elements will be much larger than the stiffness of the real continuum, for which the term Π_{dil} is vanishing.

Removal of locking. These undesirable stiffening phenomena of the displacement-based element can be partially removed with incompatible enhanced strains, which cannot be derived from compatible displacements. The form and number of these enhanced assumed strain terms determine which locking phenomena will be partially or fully removed. The advantage of a regular brick over a brick of arbitrary shape is that the static condensation process of the EAS-parameters is very simply achieved and the $\bar{\mathbf{B}}$-matrix has the same sparse structure as the conventional $\mathbf{B}$-matrix. In the following paragraphs the $\bar{\mathbf{B}}_h$-matrices and incompatible strains of some EAS-elements for linear elastic material are presented and investigated.

$\mathrm{EAS}_s^{(6)}$-element to remove shear-locking under pure bending:

$$\bar{\mathbf{B}}_{h,s}^{(6)} = \begin{bmatrix} \frac{2}{a}(s\mathbf{h}_1^T + t\mathbf{h}_2^T + st\mathbf{h}_4^T) & \mathbf{0}^T & \mathbf{0}^T \\ \mathbf{0}^T & \frac{2}{b}(r\mathbf{h}_1^T + t\mathbf{h}_3^T + rt\mathbf{h}_4^T) & \mathbf{0}^T \\ \mathbf{0}^T & \mathbf{0}^T & \frac{2}{c}(r\mathbf{h}_2^T + s\mathbf{h}_3^T + rs\mathbf{h}_4^T) \\ \frac{2}{b}(t\mathbf{h}_3^T + rt\mathbf{h}_4^T) & \frac{2}{a}(t\mathbf{h}_2^T + st\mathbf{h}_4^T) & \mathbf{0}^T \\ \frac{2}{c}(s\mathbf{h}_3^T + rs\mathbf{h}_4^T) & \mathbf{0}^T & \frac{2}{a}(s\mathbf{h}_1^T + st\mathbf{h}_4^T) \\ \mathbf{0}^T & \frac{2}{c}(r\mathbf{h}_2^T + rs\mathbf{h}_4^T) & \frac{2}{b}(r\mathbf{h}_1^T + rt\mathbf{h}_4^T) \end{bmatrix}. \tag{28}$$

Shear strains and normal strains are fully decoupled in the linear terms r, s and t. The bending–stiffness of the element is only dependent on the Poisson ratio ν, because the normal strains of the displacement element are not influenced by the incompatible shear strains $\tilde{\varepsilon}_{6,s}^i$, thus incompressibility-locking is not removed.

Incompatible shear strains with six parameters $\boldsymbol{\phi}_i$:

$$\boldsymbol{\varepsilon}^{i}_{6,s} = \begin{bmatrix} 0 \\ 0 \\ 0 \\ r\boldsymbol{\phi}_1 + s\boldsymbol{\phi}_2 \\ r\boldsymbol{\phi}_3 + t\boldsymbol{\phi}_4 \\ s\boldsymbol{\phi}_5 + t\boldsymbol{\phi}_6 \end{bmatrix}. \tag{29}$$

Compared to the displacement formulation, the bending-eigenvalues of the $EAS_s^{(6)}$-element are now exact for the case of $\nu = 0$:

(i) bending in x-direction:

$$e_1 = e_2 = \frac{E}{6}\frac{bc}{a} \xrightarrow{a \gg b,c} 0;$$

(ii) bending in y-direction:

$$e_3 = e_4 = \frac{E}{6}\frac{ac}{b} \xrightarrow{b \gg a,c} 0;$$

(iii) bending in z-direction:

$$e_5 = e_6 = \frac{E}{6}\frac{ab}{c} \xrightarrow{c \gg b,a} 0.$$

$EAS_s^{(12)}$-element to remove shear-locking:

$$\bar{\mathbf{B}}^{(12)}_{\mathrm{h},s} = \begin{bmatrix} \frac{2}{a}(s\mathbf{h}_1^{\mathrm{T}} + t\mathbf{h}_2^{\mathrm{T}} + st\mathbf{h}_4^{\mathrm{T}}) & \mathbf{0}^{\mathrm{T}} & \mathbf{0}^{\mathrm{T}} \\ \mathbf{0}^{\mathrm{T}} & \frac{2}{b}(r\mathbf{h}_1^{\mathrm{T}} + t\mathbf{h}_3^{\mathrm{T}} + rt\mathbf{h}_4^{\mathrm{T}}) & \mathbf{0}^{\mathrm{T}} \\ \mathbf{0}^{\mathrm{T}} & \mathbf{0}^{\mathrm{T}} & \frac{2}{c}(r\mathbf{h}_2^{\mathrm{T}} + s\mathbf{h}_3^{\mathrm{T}} + rs\mathbf{h}_4^{\mathrm{T}}) \\ \frac{2}{b}t\mathbf{h}_3^{\mathrm{T}} & \frac{2}{a}t\mathbf{h}_2^{\mathrm{T}} & \mathbf{0}^{\mathrm{T}} \\ \frac{2}{c}s\mathbf{h}_3^{\mathrm{T}} & \mathbf{0}^{\mathrm{T}} & \frac{2}{a}s\mathbf{h}_1^{\mathrm{T}} \\ \mathbf{0}^{\mathrm{T}} & \frac{2}{c}r\mathbf{h}_2^{\mathrm{T}} & \frac{2}{b}r\mathbf{h}_1^{\mathrm{T}} \end{bmatrix}. \tag{30}$$

Shear strains and normal strains are fully decoupled in this element. This results in a lower stiffness in complex loading situations (e.g. plate bending) than obtained for the $EAS_s^{(6)}$-element. We have to remark that a thin plate under a concentrated load or uniform loading cannot be modeled correctly with this element for $\nu > 0$ with only one layer of solid elements through the plate thickness as it is obvious that the normal strains of $EAS_s^{(12)}$ and of the pure displacement element are identical and incompressibility-locking occurs again for $\nu \to \frac{1}{2}$.

Incompatible shear strains with 12 parameters ϕ_i:

$$\boldsymbol{\varepsilon}^{i}_{(12),s} = \begin{bmatrix} 0 \\ 0 \\ 0 \\ r\phi_1 + s\phi_2 + rt\phi_3 + st\phi_4 \\ r\phi_5 + t\phi_6 + rs\phi_7 + st\phi_8 \\ s\phi_9 + t\phi_{10} + rs\phi_{11} + rt\phi_{12} \end{bmatrix}. \tag{31}$$

Remark. Another element with only constant shear strains can be generated with three additional incompatible shear strains. The corresponding $\bar{\mathbf{B}}_h$-matrix, however, then contains three zero columns and as a consequence the stiffness matrix posses three zero-energy modes, which must be stabilized. It is thus recommended to avoid such a modification of the displacement $\mathbf{B}_h$-matrix.

$EAS^{(6)}_n$-element to remove incompressibility-locking:

For this element only the normal strains of the displacement formulation are modified and the incompressibility constraint for isotropic and orthotropic materials is fulfilled; thus it is perfectly suited for volume-preserving deformations.

$$\bar{\mathbf{B}}^{(6)}_{h,n} = \begin{bmatrix} (s\mathbf{h}_1^{\mathrm{T}} + t\mathbf{h}_2^{\mathrm{T}})\frac{2}{a} & -\frac{2}{b}\frac{E_2}{E_1} r\mathbf{h}_1^{\mathrm{T}} & -\frac{2}{c}\frac{E_2}{E_1} r\mathbf{h}_2^{\mathrm{T}} \\ -\frac{2}{a}\frac{E_2}{E_1} s\mathbf{h}_1^{\mathrm{T}} & (r\mathbf{h}_1^{\mathrm{T}} + t\mathbf{h}_3^{\mathrm{T}})\frac{2}{b} & -\frac{2}{c}\frac{E_2}{E_1} s\mathbf{h}_3^{\mathrm{T}} \\ -\frac{2}{a}\frac{E_2}{E_1} t\mathbf{h}_2^{\mathrm{T}} & -\frac{2}{b}\frac{E_2}{E_1} t\mathbf{h}_3^{\mathrm{T}} & (r\mathbf{h}_2^{\mathrm{T}} + s\mathbf{h}_3^{\mathrm{T}})\frac{2}{c} \\ \frac{2}{b}(r\mathbf{h}_1^{\mathrm{T}} + t\mathbf{h}_3^{\mathrm{T}} + rt\mathbf{h}_4^{\mathrm{T}}) & \frac{2}{a}(s\mathbf{h}_1^{\mathrm{T}} + t\mathbf{h}_2^{\mathrm{T}} + st\mathbf{h}_4^{\mathrm{T}}) & \mathbf{0}^{\mathrm{T}} \\ \frac{2}{c}(r\mathbf{h}_2^{\mathrm{T}} + s\mathbf{h}_3^{\mathrm{T}} + rs\mathbf{h}_4^{\mathrm{T}}) & \mathbf{0}^{\mathrm{T}} & \frac{2}{a}(s\mathbf{h}_1^{\mathrm{T}} + t\mathbf{h}_2^{\mathrm{T}} + st\mathbf{h}_4)^{\mathrm{T}} \\ \mathbf{0}^{\mathrm{T}} & \frac{2}{c}(r\mathbf{h}_2^{\mathrm{T}} + s\mathbf{h}_3^{\mathrm{T}} + rs\mathbf{h}_4^{\mathrm{T}}) & \frac{2}{b}(r\mathbf{h}_1^{\mathrm{T}} + t\mathbf{h}_3^{\mathrm{T}} + rt\mathbf{h}_4^{\mathrm{T}}) \end{bmatrix}. \tag{32}$$

Incompatible enhanced normal strains with six parameters:

$$\boldsymbol{\varepsilon}^{i}_{6,n} = \begin{bmatrix} r\phi_1 + st\phi_2 \\ s\phi_3 + rt\phi_4 \\ t\phi_5 + rs\phi_6 \\ 0 \\ 0 \\ 0 \end{bmatrix}. \tag{33}$$

The following proof that $\mathrm{tr}(\boldsymbol{\varepsilon})$ vanishes for $\nu \to \frac{1}{2}$ is restricted here to isotropic material. The corresponding proof for orthotropic material can be performed in analogous manner, but it involves some more complex operations.

$$\varepsilon_x+\varepsilon_y+\varepsilon_z = s\frac{2}{a}\left(1-\frac{E_2}{E_1}\right)(\mathbf{h}_1^{\mathrm{T}}\mathbf{u})+t\frac{2}{a}\left(1-\frac{E_2}{E_1}\right)(\mathbf{h}_2^{\mathrm{T}}\mathbf{u})+r\frac{2}{b}\left(1-\frac{E_2}{E_1}\right)(\mathbf{h}_1^{\mathrm{T}}\mathbf{v})$$
$$+t\frac{2}{b}\left(1-\frac{E_2}{E_1}\right)(\mathbf{h}_3^{\mathrm{T}}\mathbf{v})+r\frac{2}{c}\left(1-\frac{E_2}{E_1}\right)(\mathbf{h}_2^{\mathrm{T}}\mathbf{w})-s\frac{2}{c}\left(1-\frac{E_2}{E_1}\right)(\mathbf{h}_3^{\mathrm{T}}\mathbf{w}),$$

$$\varepsilon_x+\varepsilon_y+\varepsilon_z = \left[s\frac{2}{a}(\mathbf{h}_1^{\mathrm{T}}\mathbf{u})+t\frac{2}{a}(\mathbf{h}_2^{\mathrm{T}}\mathbf{u})+r\frac{2}{b}(\mathbf{h}_1^{\mathrm{T}}\mathbf{v})+t\frac{2}{b}(\mathbf{h}_3^{\mathrm{T}}\mathbf{v})\right.$$
$$\left.+r\frac{2}{c}(\mathbf{h}_2^{\mathrm{T}}\mathbf{w})+s\frac{2}{c}(\mathbf{h}_3^{\mathrm{T}}\mathbf{w})\right]\left(1-\frac{E_2}{E_1}\right). \quad (34)$$

It remains to look at:

$$1-\frac{E_2}{E_1}=1-\frac{\nu}{1-\nu}=\frac{1-2\nu}{1-\nu}\to 0 \quad \text{for} \quad \nu\to\tfrac{1}{2}\square. \quad (35)$$

$\mathrm{EAS}_{\mathrm{n}}^{(9)}$-element to remove incompressibility-locking:

This element differs from $\mathrm{EAS}_{\mathrm{n}}^{(6)}$ only in the bilinear interpolation of the normal strains. In contrast to $\mathrm{EAS}_{\mathrm{n}}^{(6)}$, which has no bilinear normal strains, these bilinear terms are now complete. ε_x, ε_y and ε_z contain all three polynomial terms rs, rt and st.

$$\bar{\mathbf{B}}_{\mathrm{h},n}^{(9)} =$$
$$\begin{bmatrix}
\frac{2}{a}(s\mathbf{h}_1^{\mathrm{T}}+t\mathbf{h}_2^{\mathrm{T}}+st\mathbf{h}_4^{\mathrm{T}}) & -\frac{2}{b}\left(\frac{E_2}{E_1}r\mathbf{h}_1^{\mathrm{T}}+\frac{E_2}{E_1+E_2}rt\mathbf{h}_4^{\mathrm{T}}\right) & -\frac{2}{c}\left(\frac{E_2}{E_1}r\mathbf{h}_2^{\mathrm{T}}+\frac{E_2}{E_1+E_2}rs\mathbf{h}_4^{\mathrm{T}}\right)\\
-\frac{2}{a}\left(\frac{E_2}{E_1}s\mathbf{h}_1^{\mathrm{T}}+\frac{E_2}{E_1+E_2}st\mathbf{h}_4^{\mathrm{T}}\right) & \frac{2}{b}(r\mathbf{h}_1^{\mathrm{T}}+t\mathbf{h}_3^{\mathrm{T}}+rt\mathbf{h}_4^{\mathrm{T}}) & -\frac{2}{c}\left(\frac{E_2}{E_1}s\mathbf{h}_3^{\mathrm{T}}+\frac{E_2}{E_1+E_2}rs\mathbf{h}_4^{\mathrm{T}}\right)\\
-\frac{2}{a}\left(\frac{E_2}{E_1}t\mathbf{h}_2^{\mathrm{T}}+\frac{E_2}{E_1+E_2}st\mathbf{h}_4^{\mathrm{T}}\right) & -\frac{2}{b}\left(\frac{E_2}{E_1}t\mathbf{h}_3^{\mathrm{T}}+\frac{E_2}{E_1+E_2}rt\mathbf{h}_4^{\mathrm{T}}\right) & \frac{2}{c}(r\mathbf{h}_2^{\mathrm{T}}+s\mathbf{h}_3^{\mathrm{T}}+rs\mathbf{h}_4^{\mathrm{T}})\\
\frac{2}{b}(r\mathbf{h}_1^{\mathrm{T}}+t\mathbf{h}_3^{\mathrm{T}}+rt\mathbf{h}_4^{\mathrm{T}}) & \frac{2}{a}(s\mathbf{h}_1^{\mathrm{T}}+t\mathbf{h}_2^{\mathrm{T}}+st\mathbf{h}_4^{\mathrm{T}}) & \mathbf{0}^{\mathrm{T}}\\
\frac{2}{c}(r\mathbf{h}_2^{\mathrm{T}}+s\mathbf{h}_3^{\mathrm{T}}+rs\mathbf{h}_4^{\mathrm{T}}) & \mathbf{0}^{\mathrm{T}} & \frac{2}{a}(s\mathbf{h}_1^{\mathrm{T}}+t\mathbf{h}_2^{\mathrm{T}}+st\mathbf{h}_4^{\mathrm{T}})\\
\mathbf{0}^{\mathrm{T}} & \frac{2}{c}(r\mathbf{h}_2^{\mathrm{T}}+s\mathbf{h}_3^{\mathrm{T}}+rs\mathbf{h}_4^{\mathrm{T}} & \frac{2}{b}(r\mathbf{h}_1^{\mathrm{T}}+t\mathbf{h}_3^{\mathrm{T}}+rt\mathbf{h}_4^{\mathrm{T}})
\end{bmatrix}. \quad (36)$$

Incompatible enhanced normal strains with nine parameters ϕ_i:

$$\varepsilon_{9,n}^{i} = \begin{bmatrix} r\phi_1+rs\phi_2+rt\phi_3\\ s\phi_4+rs\phi_5+st\phi_6\\ t\phi_7+rt\phi_8+st\phi_9\\ 0\\ 0\\ 0 \end{bmatrix}. \quad (37)$$

Like the $\mathrm{EAS}_{\mathrm{n}}^{(6)}$-element this formulation leads to a locking free element in the case of incompressibility. The proof is also analogous to the proof for the $\mathrm{EAS}_{\mathrm{n}}^{(6)}$-element.

EAS$^{(12)}$-element to remove shear- and incompressibility-locking:

This element combines the properties of the EAS$_s^{(6)}$- and EAS$_n^{(6)}$-elements and was presented first for large deformation analysis in a very comprehensive paper by Simo *et al.* (1993).

$$\bar{\mathbf{B}}_h^{(12)} = \begin{bmatrix} (s\mathbf{h}_1^T + t\mathbf{h}_2^T)\frac{2}{a} & -\frac{2}{b}\frac{E_2}{E_1} r\mathbf{h}_1^T & -\frac{2}{c}\frac{E_2}{E_1} r\mathbf{h}_2^T \\ -\frac{2}{a}\frac{E_2}{E_1} s\mathbf{h}_1^T & (r\mathbf{h}_1^T + t\mathbf{h}_3^T)\frac{2}{b} & -\frac{2}{c}\frac{E_2}{E_1} s\mathbf{h}_3^T \\ -\frac{2}{a}\frac{E_2}{E_1} t\mathbf{h}_2^T & -\frac{2}{b}\frac{E_2}{E_1} t\mathbf{h}_3^T & (r\mathbf{h}_2^T + s\mathbf{h}_3^T)\frac{2}{c} \\ \frac{2}{b}(t\mathbf{h}_3^T + rt\mathbf{h}_4^T) & \frac{2}{a}(t\mathbf{h}_2^T + st\mathbf{h}_4^T) & \mathbf{0}^T \\ \frac{2}{c}(s\mathbf{h}_3^T + rs\mathbf{h}_4^T) & \mathbf{0}^T & \frac{2}{a}(s\mathbf{h}_1^T + st\mathbf{h}_4^T) \\ \mathbf{0}^T & \frac{2}{c}(r\mathbf{h}_2^T + rs\mathbf{h}_4^T) & \frac{2}{b}(r\mathbf{h}_1^T + rt\mathbf{h}_4^T) \end{bmatrix}. \tag{38}$$

Shear and incompressibility locking are both totally removed. The incompatible strains can be written as $\varepsilon_{12}^i = \varepsilon_{6,s}^i + \varepsilon_{6,n}^i$.

EAS$^{(21)}$-element:

This element combines the properties of the EAS$_n^{(9)}$- and EAS$_s^{(12)}$-elements. The obviously more efficient alternative, combining the EAS$_s^{(12)}$- and EAS$_n^{(6)}$-elements to develop a high-quality element, could not be chosen because the corresponding $\bar{\mathbf{B}}_h$-matrix does not contain any $\mathbf{h}_4$-vector. The consequence is that zero-energy modes would appear for the stiffness-matrix of the latter alternative.

$$\bar{\mathbf{B}}_h^{(21)} = \begin{bmatrix} \frac{2}{a}(s\mathbf{h}_1^T + t\mathbf{h}_2^T + st\mathbf{h}_4^T) & -\frac{2}{b}\left(\frac{E_2}{E_1} r\mathbf{h}_1^T + \frac{E_2}{E_1+E_2} rt\mathbf{h}_4^T\right) & -\frac{2}{c}\left(\frac{E_2}{E_1} r\mathbf{h}_2^T + \frac{E_2}{E_1+E_2} rs\mathbf{h}_4^T\right) \\ -\frac{2}{a}\left(\frac{E_2}{E_1} s\mathbf{h}_1^T + \frac{E_2}{E_1+E_2} st\mathbf{h}_4^T\right) & \frac{2}{b}(r\mathbf{h}_1^T + t\mathbf{h}_3^T + rt\mathbf{h}_4^T) & -\frac{2}{c}\left(\frac{E_2}{E_1} s\mathbf{h}_3^T + \frac{E_2}{E_1+E_2} rs\mathbf{h}_4^T\right) \\ -\frac{2}{a}\left(\frac{E_2}{E_1} t\mathbf{h}_2^T + \frac{E_2}{E_1+E_2} st\mathbf{h}_4^T\right) & -\frac{2}{b}\left(\frac{E_2}{E_1} t\mathbf{h}_3^T + \frac{E_2}{E_1+E_2} rt\mathbf{h}_4^T\right) & \frac{2}{c}(r\mathbf{h}_2^T + s\mathbf{h}_3^T + rs\mathbf{h}_4^T) \\ \frac{2}{b} t\mathbf{h}_3^T & \frac{2}{a} t\mathbf{h}_2^T & \mathbf{0}^T \\ \frac{2}{c} s\mathbf{h}_3^T & \mathbf{0}^T & \frac{2}{a} s\mathbf{h}_1^T \\ \mathbf{0}^T & \frac{2}{c} r\mathbf{h}_2^T & \frac{2}{b} r\mathbf{h}_1^T \end{bmatrix}. \tag{39}$$

The incompatible enhanced normal and shear strains are not shown, as they are given by $\varepsilon_{21}^i = \varepsilon_{12,s}^i + \varepsilon_{9,n}^i$.

EAS$^{(9)}$-element:

For completeness an element is presented that is similar to the incompatible displacement element proposed by Taylor *et al.* (1976).

$$\bar{\mathbf{B}}_{\mathrm{h}}^{(9)} = \begin{bmatrix} \frac{2}{a}(s\mathbf{h}_1^{\mathrm{T}} + t\mathbf{h}_2^{\mathrm{T}} + st\mathbf{h}_4^{\mathrm{T}}) & -\frac{2}{b}\frac{E_2}{E_1}r\mathbf{h}_1^{\mathrm{T}} & -\frac{2}{c}\frac{E_2}{E_1}r\mathbf{h}_2^{\mathrm{T}} \\ -\frac{2}{a}\frac{E_2}{E_1}s\mathbf{h}_1^{\mathrm{T}} & \frac{2}{b}(r\mathbf{h}_1^{\mathrm{T}} + t\mathbf{h}_3^{\mathrm{T}} + rt\mathbf{h}_4^{\mathrm{T}}) & -\frac{2}{c}\frac{E_2}{E_1}s\mathbf{h}_3^{\mathrm{T}} \\ -\frac{2}{a}\frac{E_2}{E_1}t\mathbf{h}_2^{\mathrm{T}} & -\frac{2}{b}\frac{E_2}{E_1}t\mathbf{h}_3^{\mathrm{T}} & \frac{2}{c}(r\mathbf{h}_2^{\mathrm{T}} + s\mathbf{h}_3^{\mathrm{T}} + rs\mathbf{h}_4^{\mathrm{T}}) \\ \frac{2}{b}(t\mathbf{h}_3^{\mathrm{T}} + rt\mathbf{h}_4^{\mathrm{T}}) & \frac{2}{a}(t\mathbf{h}_2^{\mathrm{T}} + st\mathbf{h}_4^{\mathrm{T}}) & \mathbf{0}^{\mathrm{T}} \\ \frac{2}{c}(s\mathbf{h}_3^{\mathrm{T}} + rs\mathbf{h}_4^{\mathrm{T}}) & \mathbf{0}^{\mathrm{T}} & \frac{2}{a}(s\mathbf{h}_1^{\mathrm{T}} + st\mathbf{h}_4^{\mathrm{T}}) \\ \mathbf{0}^{\mathrm{T}} & \frac{2}{c}(r\mathbf{h}_2^{\mathrm{T}} + rs\mathbf{h}_4^{\mathrm{T}}) & \frac{2}{b}(r\mathbf{h}_1^{\mathrm{T}} + rt\mathbf{h}_4^{\mathrm{T}}) \end{bmatrix}. \tag{40}$$

The incompatible enhanced normal and shear strains with nine parameters ϕ_i are:

$$\boldsymbol{\varepsilon}_9^i = \begin{bmatrix} r\phi_1 \\ s\phi_2 \\ t\phi_3 \\ r\phi_4 + s\phi_5 \\ r\phi_6 + t\phi_7 \\ s\phi_8 + t\phi_9 \end{bmatrix}. \tag{41}$$

For this element incompressibility-locking can only be suppressed if the $\mathbf{h}_4$ terms are not activated, as $\mathrm{tr}(\boldsymbol{\varepsilon})$ contains the $\mathbf{h}_4$ terms for all directions:

$$\begin{aligned} \mathrm{tr}(\boldsymbol{\varepsilon}) = \varepsilon_x + \varepsilon_y + \varepsilon_z = &\left[s\frac{2}{a}(\mathbf{h}_1^{\mathrm{T}}\mathbf{u}) + t\frac{2}{a}(\mathbf{h}_2^{\mathrm{T}}\mathbf{u}) + r\frac{2}{b}(\mathbf{h}_1^{\mathrm{T}}\mathbf{v}) + t\frac{2}{b}(\mathbf{h}_3^{\mathrm{T}}\mathbf{v}) \right. \\ &\left. + r\frac{2}{c}(\mathbf{h}_2^{\mathrm{T}}\mathbf{w}) + s\frac{2}{c}(\mathbf{h}_3^{\mathrm{T}}\mathbf{w}) \right]\left(1 - \frac{E_2}{E_1}\right) \\ &+ st(\mathbf{h}_4^{\mathrm{T}}\mathbf{u}) + rt(\mathbf{h}_4^{\mathrm{T}}\mathbf{v}) + rs(\mathbf{h}_4^{\mathrm{T}}\mathbf{w}) \\ \rightarrow\ &st(\mathbf{h}_4^{\mathrm{T}}\mathbf{u}) + rt(\mathbf{h}_4^{\mathrm{T}}\mathbf{v}) + rs(\mathbf{h}_4^{\mathrm{T}}\mathbf{w}) \quad \text{for} \quad \nu \rightarrow \tfrac{1}{2} \quad \text{[see eqn (21)]}. \end{aligned} \tag{42}$$

Other possibilities to remove locking. Another possibility to remove incompressibility-locking for all materials is to split the **B**-matrix of the displacement element in a deviatoric and a *constant* dilatational part. This procedure can be interpreted as a one-point integration of the dilatational strains:

$$\begin{aligned} \bar{\mathbf{B}} &= \mathbf{B}_{\mathrm{c,dil}} + \mathbf{B}_{\mathrm{c,dev}} + \mathbf{B}_{\mathrm{h,dev}} \\ &= \mathbf{B}_{\mathrm{c}} + \mathbf{B}_{\mathrm{h,dev}}, \end{aligned} \tag{43}$$

with

$$\mathbf{B}_{\mathrm{h,dev}} = \begin{bmatrix} \frac{4}{3a}(s\mathbf{h}_1^{\mathrm{T}} + t\mathbf{h}_2^{\mathrm{T}} + st\mathbf{h}_4^{\mathrm{T}}) & -\frac{2}{3b}(r\mathbf{h}_1^{\mathrm{T}} + t\mathbf{h}_3^{\mathrm{T}} + rt\mathbf{h}_4^{\mathrm{T}}) & -\frac{2}{3c}(r\mathbf{h}_2^{\mathrm{T}} + s\mathbf{h}_3^{\mathrm{T}} + rs\mathbf{h}_4^{\mathrm{T}}) \\ -\frac{2}{3a}(s\mathbf{h}_1^{\mathrm{T}} + t\mathbf{h}_2^{\mathrm{T}} + st\mathbf{h}_4^{\mathrm{T}}) & \frac{4}{3b}(r\mathbf{h}_1^{\mathrm{T}} + t\mathbf{h}_3^{\mathrm{T}} + rt\mathbf{h}_4^{\mathrm{T}}) & -\frac{2}{3c}(r\mathbf{h}_2^{\mathrm{T}} + s\mathbf{h}_3^{\mathrm{T}} + rs\mathbf{h}_4^{\mathrm{T}}) \\ -\frac{2}{3a}(s\mathbf{h}_1^{\mathrm{T}} + t\mathbf{h}_2^{\mathrm{T}} + st\mathbf{h}_4^{\mathrm{T}}) & -\frac{2}{3b}(r\mathbf{h}_1^{\mathrm{T}} + t\mathbf{h}_3^{\mathrm{T}} + rt\mathbf{h}_4^{\mathrm{T}}) & \frac{4}{3c}(r\mathbf{h}_2^{\mathrm{T}} + s\mathbf{h}_3^{\mathrm{T}} + rs\mathbf{h}_4^{\mathrm{T}}) \\ \frac{2}{b}(r\mathbf{h}_1^{\mathrm{T}} + t\mathbf{h}_3^{\mathrm{T}} + rt\mathbf{h}_4^{\mathrm{T}}) & \frac{2}{a}(s\mathbf{h}_1^{\mathrm{T}} + t\mathbf{h}_2^{\mathrm{T}} + st\mathbf{h}_4^{\mathrm{T}}) & \mathbf{0}^{\mathrm{T}} \\ \frac{2}{c}(r\mathbf{h}_2^{\mathrm{T}} + s\mathbf{h}_3^{\mathrm{T}} + rs\mathbf{h}_4^{\mathrm{T}}) & \mathbf{0}^{\mathrm{T}} & \frac{2}{a}(s\mathbf{h}_1^{\mathrm{T}} + t\mathbf{h}_2^{\mathrm{T}} + st\mathbf{h}_4^{\mathrm{T}}) \\ \mathbf{0}^{\mathrm{T}} & \frac{2}{c}(r\mathbf{h}_2^{\mathrm{T}} + s\mathbf{h}_3^{\mathrm{T}} + rs\mathbf{h}_4^{\mathrm{T}}) & \frac{2}{b}(r\mathbf{h}_1^{\mathrm{T}} + t\mathbf{h}_3^{\mathrm{T}} + rt\mathbf{h}_4^{\mathrm{T}}) \end{bmatrix}. \tag{44}$$

The decoupling of shear strains and normal deviatoric strains for suppressing shear-locking is achieved with the same incompatible strains as in $\mathrm{EAS}_{\mathrm{s}}^{(6)}$ or $\mathrm{EAS}_{\mathrm{s}}^{(12)}$. The formulation with $\mathrm{EAS}_{\mathrm{s}}^{(12)}$ is—for the special case of a regular brick—identical with the ADS-element of Belytschko and Bindeman (1993), which was developed without the EAS-formalism but is based on a pure $\bar{\mathbf{B}}$-method.

3.2. *Parallelepipeds*

The next step in the development of efficient elements of arbitrary shape is a parallelepiped, an element with a constant but totally filled Jacobian matrix. The effort to generate the $\bar{\mathbf{B}}_{\mathrm{h}}$-matrices is much larger than for a regular brick with sides parallel to the Cartesian coordinate axes. The time consuming static condensation procedure of the EAS-parameters can be avoided only under the condition that the elasticity-matrix is constant or is chosen to be constant within the element. The properties of the EAS-elements presented in Section 3.1, are conserved, because the incompatible and compatible strains are still aligned with each other. As an example the $\mathrm{EAS}_{\mathrm{s}}^{(6)}$-element is investigated, however, all other elements can be treated in a completely analogous manner.

In order to make the basis of the inversion of the **H**-matrix as simple as possible, the columns with identical polynomial terms in the EAS interpolation matrix **G** are arranged just beside each other:

$$\mathbf{G} = \mathbf{T}_0 \begin{bmatrix} 0 & 0 & 0 & 0 & 0 & 0 \\ 0 & 0 & 0 & 0 & 0 & 0 \\ 0 & 0 & 0 & 0 & 0 & 0 \\ r & 0 & s & 0 & 0 & 0 \\ 0 & r & 0 & 0 & t & 0 \\ 0 & 0 & 0 & s & 0 & t \end{bmatrix}$$

$$= \begin{bmatrix} r \underbrace{\begin{bmatrix} T_0^{14} & T_0^{15} \\ T_0^{24} & T_0^{25} \\ T_0^{34} & T_0^{35} \\ T_0^{44} & T_0^{45} \\ T_0^{54} & T_0^{55} \\ T_0^{64} & T_0^{65} \end{bmatrix}}_{\mathbf{T}_r} s \underbrace{\begin{bmatrix} T_0^{14} & T_0^{16} \\ T_0^{24} & T_0^{26} \\ T_0^{34} & T_0^{36} \\ T_0^{44} & T_0^{46} \\ T_0^{54} & T_0^{56} \\ T_0^{64} & T_0^{66} \end{bmatrix}}_{\mathbf{T}_s} t \underbrace{\begin{bmatrix} T_0^{15} & T_0^{16} \\ T_0^{25} & T_0^{26} \\ T_0^{35} & T_0^{36} \\ T_0^{45} & T_0^{46} \\ T_0^{55} & T_0^{56} \\ T_0^{65} & T_0^{66} \end{bmatrix}}_{\mathbf{T}_t} \end{bmatrix}. \tag{45}$$

$$\mathbf{G} = [r\mathbf{T}_r \quad s\mathbf{T}_s \quad t\mathbf{T}_t] = [\mathbf{G}_r \quad \mathbf{G}_s \quad \mathbf{G}_t], \tag{46}$$

with

$$\mathbf{G}_r, \mathbf{G}_s, \mathbf{G}_t \in R^{6\times 2} \quad \mathbf{T}_r, \mathbf{T}_s, \mathbf{T}_t \in R^{6\times 2}.$$

Therefore the **H**-matrix is block-structured:

$$\begin{aligned}\mathbf{H} &= \int_{V_e} \mathbf{G}^T\mathbf{C}\mathbf{G}\,\mathrm{d}v_e \\ &= \int_{V_e} \begin{bmatrix}\mathbf{G}_r^T \\ \mathbf{G}_s^T \\ \mathbf{G}_t^T\end{bmatrix} [\mathbf{C}\mathbf{G}_r \quad \mathbf{C}\mathbf{G}_s \quad \mathbf{C}\mathbf{G}_t]\,\mathrm{d}v_e,\end{aligned} \tag{47}$$

$$\mathbf{H} = \begin{bmatrix} \mathbf{T}_r^T\mathbf{C}\mathbf{T}_r \int_{V_e} rr\,\mathrm{d}v_e & \mathbf{T}_r^T\mathbf{C}\mathbf{T}_s \int_{V_e} rs\,\mathrm{d}v_e & \mathbf{T}_r^T\mathbf{C}\mathbf{T}_t \int_{V_e} rt\,\mathrm{d}v_e \\ \mathbf{T}_s^T\mathbf{C}\mathbf{T}_r \int_{V_e} sr\,\mathrm{d}v_e & \mathbf{T}_s^T\mathbf{C}\mathbf{T}_s \int_{V_e} ss\,\mathrm{d}v_e & \mathbf{T}_s^T\mathbf{C}\mathbf{T}_t \int_{V_e} st\,\mathrm{d}v_e \\ \mathbf{T}_t^T\mathbf{C}\mathbf{T}_r \int_{V_e} tr\,\mathrm{d}v_e & \mathbf{T}_t^T\mathbf{C}\mathbf{T}_s \int_{V_e} ts\,\mathrm{d}v_e & \mathbf{T}_t^T\mathbf{C}\mathbf{T}_t \int_{V_e} tt\,\mathrm{d}v_e \end{bmatrix}. \tag{48}$$

and because of

$$\int_{-1}^{+1}\int_{-1}^{+1}\int_{-1}^{+1} r^2 j_0\,\mathrm{d}r\,\mathrm{d}s\,\mathrm{d}t = \int_{-1}^{+1}\int_{-1}^{+1}\int_{-1}^{+1} s^2 j_0\,\mathrm{d}r\,\mathrm{d}s\,\mathrm{d}r = \int_{-1}^{+1}\int_{-1}^{+1}\int_{-1}^{+1} t^2 j_0\,\mathrm{d}r\,\mathrm{d}s\,\mathrm{d}t = \tfrac{8}{3} j_0 \tag{49}$$

$$\int_{-1}^{+1}\int_{-1}^{+1}\int_{-1}^{+1} rsj_0\,\mathrm{d}r\,\mathrm{d}s\,\mathrm{d}t = \int_{-1}^{+1}\int_{-1}^{+1}\int_{-1}^{+1} rtj_0\,\mathrm{d}r\,\mathrm{d}s\,\mathrm{d}t = \int_{-1}^{+1}\int_{-1}^{+1}\int_{-1}^{+1} stj_0\,\mathrm{d}r\,\mathrm{d}s\,\mathrm{d}t = 0,$$

H is even *block-diagonal* for a parallelepiped!

$$\mathbf{H}\begin{bmatrix} \mathbf{T}_r^T\mathbf{C}\mathbf{T}_r \frac{8}{3} j_0 & \mathbf{0} & \mathbf{0} \\ \mathbf{0} & \mathbf{T}_s^T\mathbf{C}\mathbf{T}_s \frac{8}{3} j_0 & \mathbf{0} \\ \mathbf{0} & \mathbf{0} & \mathbf{T}_t^T\mathbf{C}\mathbf{T}_t \frac{8}{3} j_0 \end{bmatrix} = \begin{bmatrix} \mathbf{H}_r & \mathbf{0} & \mathbf{0} \\ \mathbf{0} & \mathbf{H}_s & \mathbf{0} \\ \mathbf{0} & \mathbf{0} & \mathbf{H}_t \end{bmatrix}. \tag{50}$$

with

$$\mathbf{H}_r, \mathbf{H}_s, \mathbf{H}_t \in R^{2\times 2}.$$

The individual 2×2 block matrices can be inverted explicitly and independently, thus it is equally simple to set up as well the $\bar{\mathbf{B}}_h$-matrix explicitly:

$$\tilde{\mathbf{B}}^{(6)}_{\mathrm{h},s} = \mathbf{B}_\mathrm{h} - \mathbf{G}\mathbf{H}^{-1}\mathbf{L}$$

$$= \mathbf{B}_\mathrm{h} - [\mathbf{G}_r \quad \mathbf{G}_s \quad \mathbf{G}_t] \begin{bmatrix} \mathbf{H}_r^{-1} & \mathbf{0} & \mathbf{0} \\ \mathbf{0} & \mathbf{H}_s^{-1} & \mathbf{0} \\ \mathbf{0} & \mathbf{0} & \mathbf{H}_t^{-1} \end{bmatrix} \begin{bmatrix} \int_{V_\mathrm{e}} \mathbf{G}_r^\mathrm{T}\mathbf{C}\mathbf{B}_\mathrm{h}\,\mathrm{d}v_\mathrm{e} \\ \int_{V_\mathrm{e}} \mathbf{G}_s^\mathrm{T}\mathbf{C}\mathbf{B}_\mathrm{h}\,\mathrm{d}v_\mathrm{e} \\ \int_{V_\mathrm{e}} \mathbf{G}_t^\mathrm{T}\mathbf{C}\mathbf{B}_\mathrm{h}\,\mathrm{d}v_\mathrm{e} \end{bmatrix}$$

$$= \mathbf{B}_\mathrm{h} - [\mathbf{G}_r \quad \mathbf{G}_s \quad \mathbf{G}_t] \begin{bmatrix} \mathbf{H}_r^{-1}\mathbf{L}_r \\ \mathbf{H}_s^{-1}\mathbf{L}_s \\ \mathbf{H}_t^{-1}\mathbf{L}_t \end{bmatrix}$$

$$= \mathbf{B}_\mathrm{h} - \mathbf{G}_r\mathbf{H}_r^{-1}\mathbf{L}_r - \mathbf{G}_s\mathbf{H}_s^{-1}\mathbf{L}_s - \mathbf{G}_t\mathbf{H}_t^{-1}\mathbf{L}_t, \tag{51}$$

with: $\mathbf{L}_r, \mathbf{L}_s, \mathbf{L}_t \in \mathbf{R}^{2\times 24}$

$$\tilde{\mathbf{B}}^{(6)}_{\mathrm{h},s} = \mathbf{B}_\mathrm{h} - r\mathbf{T}_r\mathbf{H}_r^{-1}\mathbf{T}_r^\mathrm{T}\int_{V_\mathrm{e}} \mathbf{C}\mathbf{B}_\mathrm{h} r\,\mathrm{d}v_\mathrm{e}$$

$$- s\mathbf{T}_s\mathbf{H}_s^{-1}\mathbf{T}_s^\mathrm{T}\int_{V_\mathrm{e}} \mathbf{C}\mathbf{B}_\mathrm{h} s\,\mathrm{d}v_\mathrm{e}$$

$$- t\mathbf{T}_t\mathbf{H}_t^{-1}\mathbf{T}_t^\mathrm{T}\int_{V_\mathrm{e}} \mathbf{C}\mathbf{B}_\mathrm{h} t\,\mathrm{d}v_\mathrm{e}, \tag{52}$$

$$\tilde{\mathbf{B}}^{(6)}_{\mathrm{h},s} = \mathbf{B}_\mathrm{h} - r(\mathbf{T}_r\mathbf{H}_r^{-1}\mathbf{T}_r^\mathrm{T})\bar{\mathbf{L}}_r$$

$$- s(\mathbf{T}_s\mathbf{H}_s^{-1}\mathbf{T}_s^\mathrm{T})\bar{\mathbf{L}}_s$$

$$- t(\mathbf{T}_t\mathbf{H}_t^{-1}\mathbf{T}_t^\mathrm{T})\bar{\mathbf{L}}_t, \tag{53}$$

$$\tilde{\mathbf{B}}^{(6)}_{\mathrm{h},s} = \mathbf{B}_h - r\mathbf{B}_r - s\mathbf{B}_s - t\mathbf{B}_t \quad \text{with} \quad \mathbf{B}_q = \mathbf{T}_q\mathbf{H}^{-1}\mathbf{T}_q^\mathrm{T}\bar{\mathbf{L}}_q \quad (q = r, s, t). \tag{54}$$

The effort can be further substantially reduced by avoiding the unnecessary numerical integration of the three matrices $\bar{\mathbf{L}}_r$, $\bar{\mathbf{L}}_s$ and $\bar{\mathbf{L}}_t$. These matrices can be integrated symbolically without any difficulties, because the integrands are simple polynomials in local element coordinates, a fact Belytschko and Wang (1987) demonstrated in context with Hellinger–Reissner elements.

$$\bar{\mathbf{L}}_r = \tfrac{8}{3} j_0 \mathbf{C} \begin{bmatrix} j_{12}^{-1}\mathbf{h}_1^\mathrm{T} + j_{13}^{-1}\mathbf{h}_2^\mathrm{T} & \mathbf{0}^\mathrm{T} & \mathbf{0}^\mathrm{T} \\ \mathbf{0}^\mathrm{T} & j_{22}^{-1}\mathbf{h}_1^\mathrm{T} + j_{23}^{-1}\mathbf{h}_2^\mathrm{T} & \mathbf{0}^\mathrm{T} \\ \mathbf{0}^\mathrm{T} & \mathbf{0}^\mathrm{T} & j_{32}^{-1}\mathbf{h}_1^\mathrm{T} + j_{33}^{-1}\mathbf{h}_2^\mathrm{T} \\ j_{22}^{-1}\mathbf{h}_1^\mathrm{T} + j_{23}^{-1}\mathbf{h}_2^\mathrm{T} & j_{12}^{-1}\mathbf{h}_1^\mathrm{T} + j_{13}^{-1}\mathbf{h}_2^\mathrm{T} & \mathbf{0}^\mathrm{T} \\ j_{32}^{-1}\mathbf{h}_1^\mathrm{T} + j_{33}^{-1}\mathbf{h}_2^\mathrm{T} & \mathbf{0}^\mathrm{T} & j_{12}^{-1}\mathbf{h}_1^\mathrm{T} + j_{13}^{-1}\mathbf{h}_2^\mathrm{T} \\ \mathbf{0}^\mathrm{T} & j_{32}^{-1}\mathbf{h}_1^\mathrm{T} + j_{33}^{-1}\mathbf{h}_2^\mathrm{T} & j_{22}^{-1}\mathbf{h}_1^\mathrm{T} + j_{23}^{-1}\mathbf{h}_2^\mathrm{T} \end{bmatrix}, \tag{55}$$

$$\bar{\mathbf{L}}_s = \tfrac{8}{3} j_0 \mathbf{C} \begin{bmatrix} j_{11}^{-1}\mathbf{h}_1^{\mathrm{T}} + j_{13}^{-1}\mathbf{h}_3^{\mathrm{T}} & \mathbf{0}^{\mathrm{T}} & \mathbf{0}^{\mathrm{T}} \\ \mathbf{0}^{\mathrm{T}} & j_{21}^{-1}\mathbf{h}_1^{\mathrm{T}} + j_{23}^{-1}\mathbf{h}_3^{\mathrm{T}} & \mathbf{0}^{\mathrm{T}} \\ \mathbf{0}^{\mathrm{T}} & \mathbf{0}^{\mathrm{T}} & j_{31}^{-1}\mathbf{h}_1^{\mathrm{T}} + j_{33}^{-1}\mathbf{h}_3^{\mathrm{T}} \\ j_{21}^{-1}\mathbf{h}_1^{\mathrm{T}} + j_{23}^{-1}\mathbf{h}_3^{\mathrm{T}} & j_{11}^{-1}\mathbf{h}_1^{\mathrm{T}} + j_{13}^{-1}\mathbf{h}_3^{\mathrm{T}} & \mathbf{0}^{\mathrm{T}} \\ j_{31}^{-1}\mathbf{h}_1^{\mathrm{T}} + j_{33}^{-1}\mathbf{h}_3^{\mathrm{T}} & \mathbf{0}^{\mathrm{T}} & j_{11}^{-1}\mathbf{h}_1^{\mathrm{T}} + j_{13}^{-1}\mathbf{h}_3^{\mathrm{T}} \\ \mathbf{0}^{\mathrm{T}} & j_{31}^{-1}\mathbf{h}_1^{\mathrm{T}} + j_{33}^{-1}\mathbf{h}_3^{\mathrm{T}} & j_{21}^{-1}\mathbf{h}_1^{\mathrm{T}} + j_{23}^{-1}\mathbf{h}_3^{\mathrm{T}} \end{bmatrix}, \tag{56}$$

$$\bar{\mathbf{L}}_t = \tfrac{8}{3} j_0 \mathbf{C} \begin{bmatrix} j_{11}^{-1}\mathbf{h}_2^{\mathrm{T}} + j_{12}^{-1}\mathbf{h}_3^{\mathrm{T}} & \mathbf{0}^{\mathrm{T}} & \mathbf{0}^{\mathrm{T}} \\ \mathbf{0}^{\mathrm{T}} & j_{21}^{-1}\mathbf{h}_2^{\mathrm{T}} + j_{22}^{-1}\mathbf{h}_3^{\mathrm{T}} & \mathbf{0}^{\mathrm{T}} \\ \mathbf{0}^{\mathrm{T}} & \mathbf{0}^{\mathrm{T}} & j_{31}^{-1}\mathbf{h}_2^{\mathrm{T}} + j_{32}^{-1}\mathbf{h}_3^{\mathrm{T}} \\ j_{21}^{-1}\mathbf{h}_2^{\mathrm{T}} + j_{22}^{-1}\mathbf{h}_3^{\mathrm{T}} & j_{11}^{-1}\mathbf{h}_2^{\mathrm{T}} + j_{12}^{-1}\mathbf{h}_3^{\mathrm{T}} & \mathbf{0}^{\mathrm{T}} \\ j_{31}^{-1}\mathbf{h}_2^{\mathrm{T}} + j_{32}^{-1}\mathbf{h}_3^{\mathrm{T}} & \mathbf{0}^{\mathrm{T}} & j_{11}^{-1}\mathbf{h}_2^{\mathrm{T}} + j_{12}^{-1}\mathbf{h}_3^{\mathrm{T}} \\ \mathbf{0}^{\mathrm{T}} & j_{31}^{-1}\mathbf{h}_2^{\mathrm{T}} + j_{32}^{-1}\mathbf{h}_3^{\mathrm{T}} & j_{21}^{-1}\mathbf{h}_2^{\mathrm{T}} + j_{22}^{-1}\mathbf{h}_3^{\mathrm{T}} \end{bmatrix}. \tag{57}$$

The major disadvantage of a parallelepiped compared to a regular brick is the computation of the completely filled 6×24 matrices $\mathbf{B}_r$, $\mathbf{B}_s$ and $\mathbf{B}_t$, which requires a considerable number of matrix-multiplications. A further disadvantage is the loss of the sparse structure of the displacement $\mathbf{B}_{\mathrm{h}}$-matrix. In contrast to many $\bar{\mathbf{B}}$ formulations, however, the properties of EAS-elements are totally conserved by the change from a regular brick connected to a local orthogonal system to a parallelepiped, the latter connected to a locally *skewed*, position independent coordinate system.

Remark. For the EAS$^{(21)}$-element the effort is considerable even for a parallelepiped, because it is necessary to invert three 4×4 and three 3×3 block matrices.

3.3. *Hexahedral elements of arbitrary shape*

Elements, which have neither the shape of a brick or parallelepiped, are difficult to investigate, because their Jacobian matrix is coordinate dependent. The **H**-matrix is totally filled and therefore the set-up of the $\bar{\mathbf{B}}_{\mathrm{h}}$-matrix requires the inversion of a 6×6 up to a 21×21-matrix depending on the number of enhanced strains. The enormous increase in effort, however, is not followed by an equivalent growth in quality justifying these additional costs, because the quality of every element, independent on any special formulation, decreases rapidly with increasing deviation from rectangular shape. The enhanced assumed strain formulation has another disadvantage—compatible and enhanced strains do not correspond to each other any more for arbitrary shapes, so locking occurs again. The reason for this behavior is the transformation of the incompatible strains $e_{ij}^{(i)}$ with respect to local or natural coordinates to components $\boldsymbol{\varepsilon}_{ij}^{(i)}$ with respect to Cartesian coordinates. The transformation is not performed point-wise, but only at the element origin. This corresponds to a change from a skewed but position independent basis to a Cartesian basis.

$$\boldsymbol{\varepsilon}_{kl}^{(i)} = \frac{j_0}{\det} \frac{\partial \xi^i}{\partial x_{(0)}^k} e_{ij}^{(i)} \frac{\partial \xi^j}{\partial x_{(0)}^l} = \frac{j_0}{\det} j_{ki(0)}^{-1} e_{ij}^{(i)} j_{lj(0)}^{-1}. \tag{58}$$

$j_{ki}^{-1} = \partial \xi^i / \partial x^k$, $(i, k = 1, \ldots, 3)$ are the elements of the inverse Jacobian matrix $\mathbf{J}^{-1}$, j_0 and det are the Jacobians at the element origin, respectively, at any point ξ.

For the position-dependent compatible strains the shape-function derivatives with respect to Cartesian coordinates have to be determined:

$$\nabla_x N_h^i = \mathbf{J}_{(\xi)}^{-1} \nabla_\xi N_h^i$$
$$= \mathbf{J}_{(\xi)}^{-1} \nabla_\xi (rs\gamma_1^i + rt\gamma_2^i - st\gamma_3^i + rst\gamma_4^i). \tag{59}$$

In the very first formulation of Simo and Rifai (1990) the gradients of the shape-function N_h^i with respect to natural coordinates are transformed point-wise using the inverse Jacobian matrix to gradients in Cartesian coordinates. Because the EAS-interpolation terms are selected in the reference-system only for a regular brick (see Section 3.1), the transformation of compatible displacement-gradients and enhanced strains is different and therefore the two different strain fields cannot correspond with respect to remove locking. Simo *et al.* (1993) modified the gradients of the shape-functions for this reason to:

$$\nabla_x N_h^i = \frac{j_0}{\det} J_{(0)}^{-1} \nabla_\xi N_h^i. \tag{60}$$

This modification has the undesirable consequence that the element is no longer able to represent all constant stress- or strain-states exactly, thus the "patch-test" is not exactly satisfied and therefore convergence difficulties may occur. Furthermore, there is only a slight increase in efficiency compared to the first EAS-formulation (Simo and Rifai, 1990), because the **H**-matrix is totally filled even for a constant elasticity-matrix **C** and therefore the static condensation of 6 up to 21 EAS-parameters is necessary.

3.4. *New proposed elements*

In order to avoid the static condensation for arbitrarily formed elements it is not sufficient to operate only with a block-diagonal **H**-matrix like for Hellinger–Reissner elements, see Sze (1992), Belytschko and Wang (1987). Without a simultaneous modification of the interpolation matrices for position dependent compatible ($\mathbf{B}_h$) and enhanced incompatible (**G**) strains, slight locking occurs. The integration-rule of the element-stiffness matrix and internal nodal-force vector must be modified too, otherwise the patch-test for arbitrarily formed elements cannot be fulfilled.

All the described difficulties to develop an *efficient and accurate* eight-node solid element can be removed by firstly splitting up the stiffness-matrix into a matrix $\mathbf{K}_{conv}$, which ensures convergence, and a stabilization matrix $\mathbf{K}_{stab}$, and secondly introducing modifications into the submatrices:

$$\mathbf{K}_{e,mod} = \mathbf{K}_{conv} + \mathbf{K}_{stab}, \tag{61}$$

$$\mathbf{K}_{stab} = \int_{-1}^{+1}\int_{-1}^{+1}\int_{-1}^{+1} \mathbf{B}_{h,mod}^T \mathbf{C} \mathbf{B}_{h,mod}\, j_0 \,dr\,ds\,dt - \mathbf{L}_{mod}^T \mathbf{H}_{mod}^{-1} \mathbf{L}_{mod}$$
$$= \int_{-1}^{+1}\int_{-1}^{+1}\int_{-1}^{+1} \bar{\mathbf{B}}_{h,mod}^T \mathbf{C} \bar{\mathbf{B}}_{h,mod}\, j_0 \,dr\,ds\,dt. \tag{62}$$

For the computation of $\mathbf{K}_{stab}$ the Jacobian-matrix and the Jacobian-determinant are evaluated only at the *element-origin*. The $\bar{\mathbf{B}}_{h,mod}$-matrices are therefore identical with the $\bar{\mathbf{B}}_h$-matrices presented in Section 3.2 except for one important difference: in order to avoid rank-deficiencies of the stiffness matrix the **h**-vectors in the $\mathbf{B}_{h,mod}$-matrix must be substituted by the γ-vectors, see eqn (4).

It is also necessary to determine a proper matrix $\mathbf{K}_{conv}$, which ensures convergence. In opposite to the two-dimensional four-node solid element, the constant matrix $\mathbf{B}_c$ of an arbitrarily formed element alone is not sufficient to compute the internal nodal-force vector $\mathbf{f}_{int}$ of a constant stress-state $\boldsymbol{\sigma}_c$ correctly:

$$\mathbf{f}_{\text{int}} = \int_{V_e} (\mathbf{B}_c^T + \mathbf{B}_h^T)\boldsymbol{\sigma}_c \, dv_e$$

$$= \mathbf{B}_c^T \boldsymbol{\sigma}_c V_e + \int_{V_e} \mathbf{B}_h \, dv_e \boldsymbol{\sigma}_c \neq 8 j_0 \mathbf{B}_c^T \boldsymbol{\sigma}_c. \tag{63}$$

A strain–displacement matrix $\hat{\mathbf{B}}_c$, with which $\mathbf{f}_{\text{int}}$ is computed correctly in the case of a homogenous stress-state, was first suggested by Flanagan and Belytschko (1981) in their investigation of a "uniform strain hexahedron":

$$\hat{\mathbf{B}}_c = \mathbf{B}_c + \frac{1}{V_e}\int_{V_e} \mathbf{B}_h \, dv_e = \frac{1}{V_e}\int_{V_e} \mathbf{B} \, dv_e. \tag{64}$$

Using $\hat{\mathbf{B}}_c$ the rank-six matrix $\mathbf{K}_{\text{conv}}$ can now be written in a simple form, which in the case of a parallelepiped ($\int_{v_e} \mathbf{B}_h \, dV_e = 0$!) reduces to the well-known one-point integrated matrix:

$$\mathbf{K}_{\text{conv}} = \hat{\mathbf{B}}_c^T \mathbf{C} \hat{\mathbf{B}}_c V_e = \frac{1}{V_e}\int_{V_e} \mathbf{B}^T \, dv_e \mathbf{C} \int_{V_e} \mathbf{B} \, dv_e. \tag{65}$$

Discussion. The modified element-stiffness matrix $\mathbf{K}_{e,\text{mod}}$ is a good approximation for element shapes with only slight deviations from regular brick or parallelepipedic geometry. For elements with strongly distorted shapes, which a professional mesh-generator should avoid anyway, no results can be expected which are comparable to the results obtained with a regular brick independent of any special formulation (HR-, EAS- or pure displacement-method). Stiffness-matrices and nodal-force vectors should therefore be set up with as little effort as possible and at least should represent constant stress states correctly. These demands are fully satisfied by the presented element formulation.

4. NUMERICAL EXAMPLES

The numerical examples are chosen to qualify the developed elements for arbitrary situations.

4.1. *Patch test*

All the described elements satisfy the seven element patch-test proposed by Belytschko and Bindeman (1993). This mesh is sufficiently distorted for convergence tests in the case of hexahedral elements with arbitrary shape.

4.2. *Eigenvalue analysis of a single element*

This eigenvalue analysis proposed as a single element-test by Simo *et al.* (1993) and Andelfinger and Ramm (1993) is used to assess the performance in the near incompressible limit. The requirement for proper element behavior in the incompressible regime is that only one single eigenvalue goes to infinity, when the Poisson ratio ν goes to $\frac{1}{2}$, thus the element does not show so-called incompressibility-locking.

The analysis here is restricted to isotropic linear elastic material with an elasticity modulus $E = 1.0$ and the incompressibility constraint is enforced by a Poisson ratio of $\nu = 0.4999$. The non-zero eigenvalues for all elements investigated are given in the following tables. The critical eigenvalues which give information about locking are bold printed. In

Table 1. Eigenvalues for the undistorted unit cube

Number	Disp	HR	$EAS_n^{(6)}$	$EAS^{(9)}$	$EAS^{(12)}$	$EAS^{(21)}$
7	0.55556×10^{-1}	0.55555×10^{-1}	0.37037×10^{-1}	0.55556×10^{-1}	0.37037×10^{-1}	0.55555×10^{-1}
8	0.55556×10^{-1}	0.55555×10^{-1}	0.37037×10^{-1}	0.55556×10^{-1}	0.37037×10^{-1}	0.55555×10^{-1}
9	0.16667×10^{0}	0.55555×10^{-1}	0.37037×10^{-1}	0.11111×10^{0}	0.37037×10^{-1}	0.55555×10^{-1}
10	0.16667×10^{0}	0.55556×10^{-1}	0.55556×10^{-1}	0.11111×10^{0}	0.55556×10^{-1}	0.55556×10^{-1}
11	0.16667×10^{0}	0.55556×10^{-1}	0.55556×10^{-1}	0.11111×10^{0}	0.55556×10^{-1}	0.55556×10^{-1}
12	0.22222×10^{0}	0.11111×10^{0}	0.16667×10^{0}	0.22222×10^{0}	0.11111×10^{0}	0.11111×10^{0}
13	*0.33334×10^{0}*	0.11111×10^{0}	0.16667×10^{0}	0.33333×10^{0}	0.11111×10^{0}	0.11111×10^{0}
14	*0.33334×10^{0}*	0.11111×10^{0}	0.16667×10^{0}	0.33333×10^{0}	0.11111×10^{0}	0.11111×10^{0}
15	*0.33334×10^{0}*	0.22222×10^{0}	0.22222×10^{0}	0.33333×10^{0}	0.22222×10^{0}	0.22222×10^{0}
16	*0.33334×10^{0}*	0.33333×10^{0}	*0.33334×10^{0}*	0.33334×10^{0}	0.33333×10^{0}	0.33333×10^{0}
17	*0.33334×10^{0}*	0.33333×10^{0}	*0.33334×10^{0}*	*0.33334×10^{0}*	0.33333×10^{0}	0.33333×10^{0}
18	**0.92473×10^{3}**	0.33333×10^{0}	*0.33334×10^{0}*	*0.33334×10^{0}*	0.33333×10^{0}	0.33333×10^{0}
19	**0.92473×10^{3}**	*0.33334×10^{0}*	*0.33334×10^{0}*	*0.33334×10^{0}*	*0.33334×10^{0}*	*0.33334×10^{0}*
20	**0.92473×10^{3}**	*0.33334×10^{0}*	*0.33334×10^{0}*	*0.33334×10^{0}*	*0.33334×10^{0}*	*0.33334×10^{0}*
21	**0.55481×10^{4}**	*0.33334×10^{0}*	0.38888×10^{0}	**0.92473×10^{3}**	*0.33334×10^{0}*	*0.33334×10^{0}*
22	**0.55481×10^{4}**	*0.33334×10^{0}*	0.38888×10^{0}	**0.92473×10^{3}**	*0.33334×10^{0}*	*0.33334×10^{0}*
23	**0.55481×10^{4}**	*0.33334×10^{0}*	0.38888×10^{0}	**0.92473×10^{3}**	*0.33334×10^{0}*	*0.33334×10^{0}*
24	*0.24966×10^{5}*	*0.24966×10^{5}*	*0.24966×10^{5}*	*0.24966×10^{5}*	*0.24966×10^{5}*	*0.24966×10^{5}*

Tables 1 and 2 the eigenvalues of an undistorted unit cube and a strongly distorted cube (see Fig. 2), using standard eight-point integration and full static condensation of the internal variables, are compared for all investigated elements. The six eigenvalues of the constant strain-states, which are identical for all element formulations are printed in Table 1 in italic letters. Their corresponding eigenmodes can be identified as three shear modes, two tension modes and the dilatational mode.

The following abbreviations are used: Disp is the pure displacement element. HR is the 12-parameter Hellinger–Reissner element with independent assumptions for the stresses, which has been proven by many authors as the most accurate element in the linear elastic regime. $EAS_n^{(6)}$, $EAS^{(9)}$, $EAS^{(12)}$ and $EAS^{(21)}$ are the enhanced strain elements as presented in Section 3.1.

In Table 3 eigenvalues of the strongly distorted cube are given for the newly developed, so-called modified elements described in Section 3.4.

Looking at the results, we obtain that for the undistorted cube (Table 1) the pure displacement element Disp has seven very large eigenvalues and the $EAS^{(9)}$-element has a total of four eigenvalues in this regime. These observations are in agreement with the expected locking behavior of the displacement formulation and the prescribed deficiencies of the $EAS^{(9)}$-element which do not satisfy the incompressibility constraint (see Section

Table 2. Eigenvalues for the distorted cube, all elements with standard formulation

Number	Disp	HR	$EAS_n^{(6)}$	$EAS^{(9)}$	$EAS^{(12)}$	$EAS^{(21)}$
7	0.29383×10^{0}	0.14718×10^{-1}	0.75300×10^{-1}	0.24498×10^{0}	0.74700×10^{-1}	0.93081×10^{-1}
8	0.36803×10^{0}	0.79644×10^{-1}	0.17320×10^{0}	0.26252×10^{0}	0.15690×10^{0}	0.10839×10^{0}
9	0.39467×10^{0}	0.87180×10^{-1}	0.21379×10^{0}	0.33299×10^{0}	0.16762×10^{0}	0.19745×10^{0}
10	0.56507×10^{0}	0.23546×10^{0}	0.34049×10^{0}	0.41845×10^{0}	0.27878×10^{0}	0.25324×10^{0}
11	0.62894×10^{0}	0.24358×10^{0}	0.38971×10^{0}	0.44851×10^{0}	0.31913×10^{0}	0.29189×10^{0}
12	0.79480×10^{0}	0.29301×10^{0}	0.42885×10^{0}	0.52240×10^{0}	0.40637×10^{0}	0.33925×10^{0}
13	0.82133×10^{0}	0.36654×10^{0}	0.58489×10^{0}	0.70751×10^{0}	0.43031×10^{0}	0.38111×10^{0}
14	0.93235×10^{0}	0.51686×10^{0}	0.61499×10^{0}	0.75886×10^{0}	0.56994×10^{0}	0.48216×10^{0}
15	0.11044×10^{1}	0.59858×10^{0}	0.79551×10^{0}	0.85731×10^{0}	0.69500×10^{0}	0.63385×10^{0}
16	0.12870×10^{1}	0.63981×10^{0}	0.86302×10^{0}	0.11775×10^{1}	0.72835×10^{0}	0.70247×10^{0}
17	**0.47862×10^{3}**	0.69282×10^{0}	0.89948×10^{0}	0.12629×10^{1}	0.88342×10^{0}	0.83881×10^{0}
18	**0.23570×10^{4}**	0.94220×10^{0}	0.11343×10^{1}	0.15033×10^{1}	0.98909×10^{0}	0.86905×10^{0}
19	**0.31004×10^{4}**	0.95245×10^{0}	0.12738×10^{1}	0.20848×10^{1}	0.12611×10^{1}	0.11786×10^{1}
20	**0.11894×10^{5}**	0.12308×10^{1}	0.17411×10^{1}	**0.53017×10^{3}**	0.14608×10^{1}	0.14096×10^{1}
21	**0.15221×10^{5}**	0.13825×10^{1}	0.31269×10^{1}	**0.51665×10^{4}**	0.30197×10^{1}	0.16296×10^{1}
22	**0.26958×10^{5}**	0.21433×10^{1}	0.37010×10^{1}	**0.54145×10^{4}**	0.35457×10^{1}	0.19427×10^{1}
23	**0.29834×10^{5}**	0.23588×10^{1}	**0.11935×10^{4}**	**0.12278×10^{5}**	**0.11935×10^{4}**	**0.11938×10^{4}**
24	**0.77793×10^{5}**	**0.74004×10^{5}**	**0.74004×10^{5}**	**0.74298×10^{5}**	**0.74004×10^{5}**	**0.74004×10^{5}**

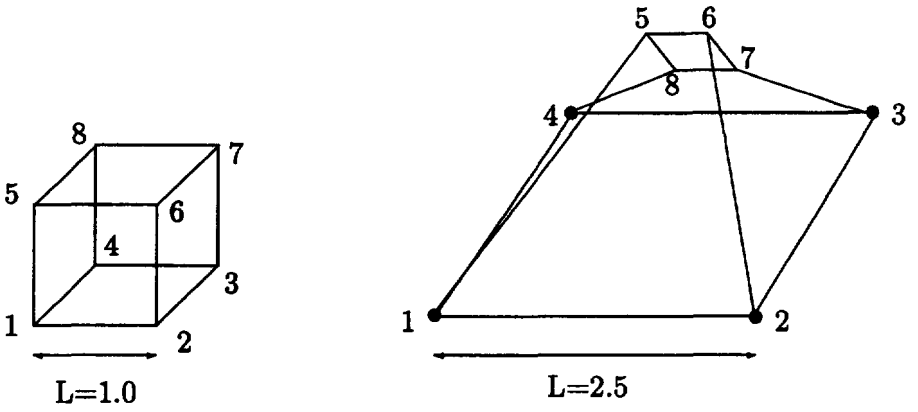

$$x_c = (-2.5, +2.5, +2.5, -2.5, -0.5, +0.5, +0.5, -0.5)^T$$
$$y_c = (-2.5, -2.5, +2.5, +2.5, -2.5, -2.5, +2.5, +2.5)^T$$
$$z_c = (-1.5, -1.5, -0.5, -0.5, +1.5, +1.5, +0.5, +0.5)^T$$

Fig. 2. Undistorted unit cube and strongly distorted element.

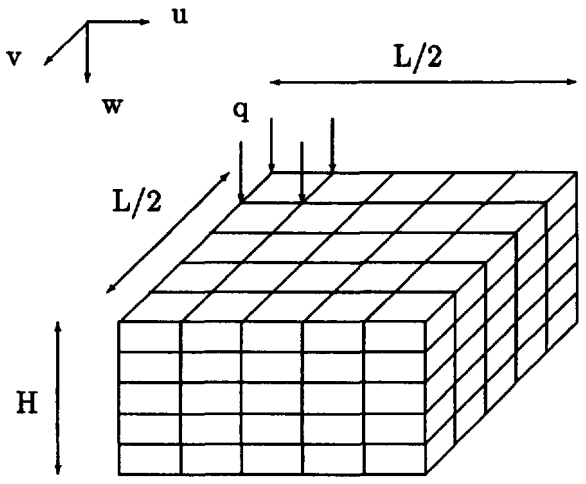

Fig. 3. Regular block loaded by a uniform pressure load q acting on an area of 20×20 in the center ($H = 50$, $L/2 = 50$, only one quarter of the block is modeled).

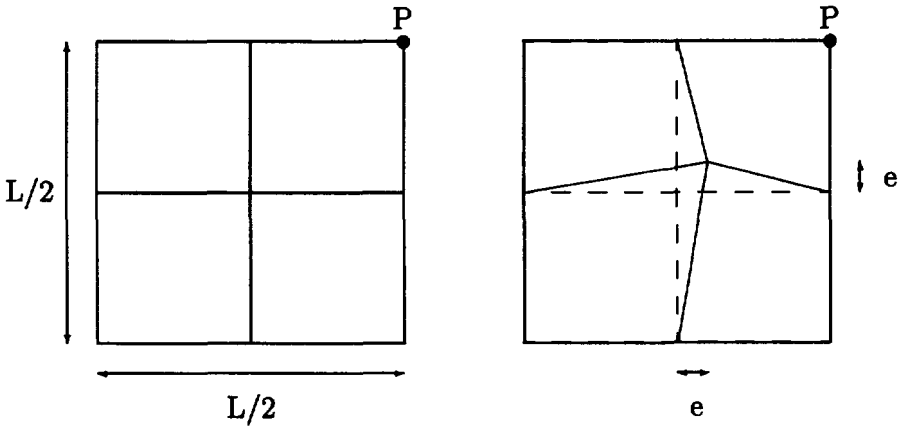

Fig. 4. Clamped plate loaded by concentrated force P; only one quarter is shown ($L/2 = 50$, $e = 10$).

Table 3. Eigenvalues for the distorted cube, all elements with the suggested modifications

Number	Disp-mod	HR-mod	$EAS_n^{(6)}$-mod	$EAS^{(9)}$-mod	$EAS^{(12)}$-mod	$EAS^{(21)}$-mod
7	0.82392×10^{-1}	0.82375×10^{-1}	0.74074×10^{-1}	0.82375×10^{-1}	0.74074×10^{-1}	0.82375×10^{-1}
8	0.35619×10^{0}	0.11111×10^{0}	0.82392×10^{-1}	0.24751×10^{0}	0.82375×10^{-1}	0.11111×10^{0}
9	0.39444×10^{0}	0.11111×10^{0}	0.12037×10^{0}	0.29039×10^{0}	0.12037×10^{0}	0.11111×10^{0}
10	0.40941×10^{0}	0.24751×10^{0}	0.12037×10^{0}	0.29438×10^{0}	0.12037×10^{0}	0.24751×10^{0}
11	0.44879×10^{0}	0.25000×10^{0}	0.35602×10^{0}	0.35813×10^{0}	0.24751×10^{0}	0.25000×10^{0}
12	0.52176×10^{0}	0.29039×10^{0}	0.37589×10^{0}	0.48226×10^{0}	0.29039×10^{0}	0.29039×10^{0}
13	0.85668×10^{0}	0.29438×10^{0}	0.38645×10^{0}	0.66472×10^{0}	0.29438×10^{0}	0.29438×10^{0}
14	0.92792×10^{0}	0.35813×10^{0}	0.42902×10^{0}	0.69124×10^{0}	0.35813×10^{0}	0.35813×10^{0}
15	0.93329×10^{0}	0.48226×10^{0}	0.50386×10^{0}	0.90600×10^{0}	0.48226×10^{0}	0.48226×10^{0}
16	0.11683×10^{1}	0.66472×10^{0}	0.76758×10^{0}	0.91432×10^{0}	0.66472×10^{0}	0.66472×10^{0}
17	0.12832×10^{1}	0.69124×10^{0}	0.84647×10^{0}	0.12047×10^{1}	0.69124×10^{0}	0.69124×10^{0}
18	$\mathbf{0.18495 \times 10^{4}}$	0.90600×10^{0}	0.91732×10^{0}	0.14635×10^{1}	0.90600×10^{0}	0.90600×10^{0}
19	$\mathbf{0.18495 \times 10^{4}}$	0.91432×10^{0}	0.99923×10^{0}	0.17072×10^{1}	0.91432×10^{0}	0.91432×10^{0}
20	$\mathbf{0.41612 \times 10^{4}}$	0.12047×10^{1}	0.12213×10^{1}	0.19566×10^{1}	0.12047×10^{1}	0.12047×10^{1}
21	$\mathbf{0.16252 \times 10^{5}}$	0.14635×10^{1}	0.17367×10^{1}	$\mathbf{0.18495 \times 10^{4}}$	0.14635×10^{1}	0.14635×10^{1}
22	$\mathbf{0.23580 \times 10^{5}}$	0.17072×10^{1}	0.18436×10^{1}	$\mathbf{0.18495 \times 10^{4}}$	0.17072×10^{1}	0.17072×10^{1}
23	$\mathbf{0.24901 \times 10^{5}}$	0.19566×10^{1}	0.21193×10^{1}	$\mathbf{0.41612 \times 10^{4}}$	0.19566×10^{1}	0.18566×10^{1}
24	$\mathbf{0.76967 \times 10^{5}}$	$\mathbf{0.74004 \times 10^{5}}$	$\mathbf{0.74004 \times 10^{5}}$	$\mathbf{0.74004 \times 10^{5}}$	$\mathbf{0.74004 \times 10^{5}}$	$\mathbf{0.74004 \times 10^{5}}$

Table 4. Vertical center displacement w_c of the regular block

Element type	HR	Disp	Disp/P0	$EAS_n^{(6)}$	$EAS^{(9)}$	$EAS^{(12)}$	$EAS^{(21)}$
w_c	0.019	0.0016	0.0197	0.0186	0.011	0.019	0.019

3.1). The other elements HR, $EAS_n^{(6)}$, $EAS^{(12)}$, $EAS^{(21)}$ have only one very large eigenvalue, which correctly corresponds to the dilatational mode.

The distortion of the cube results in an element stiffening for all fully integrated elements except for the HR-element, with independent assumptions for the stresses. There is one more very large eigenvalue visible indicating a second but incorrect dilatational mode for the elements $EAS_n^{(6)}$, $EAS^{(12)}$ and $EAS^{(21)}$. For the elements $EAS^{(9)}$ and Disp, both already giving improper results for the undistorted cube, there is an additional fifth and eighth, respectively, very large eigenvalue in the incompressible limit. The additional critical value for $EAS^{(9)}$ is a direct consequence of the non-corresponding compatible and incompatible enhanced strains for elements with arbitrary shape, as described in Section 3.3. With the newly developed modified elements these severe locking phenomena are removed, as indicated in Table 3, because enhanced strains and compatible strains are again corresponding correctly.

4.3. *Regular block with incompressible material*

This typical problem for soil and geomechanics shows to some extent the influence of the incompressibility-locking on the displacements; bending and shear action is not present in the example. It belongs to Andelfinger's and Ramm's (1993) examples catalogue. A regular block with side-lengths of 100 and a height of 50, which is fixed at the bottom is loaded at the top by a uniform pressure load of $q = 250$ unit area^{-1} acting on an area of 20×20 at the center. For symmetry reasons only one quarter of the block is modeled with a uniform $5 \times 5 \times 5$ element mesh with the corresponding symmetry boundary conditions. The material parameters $E = 210000$ and $\nu = 0.4999$ are chosen to enforce the incompressibility constraint.

In Table 4 the vertical center displacements for different element formulations are shown. The elements HR, $EAS^{(12)}$, $EAS^{(21)}$ and the element with one-point integration for the dilatational stiffness named Disp/P0 are free of locking, and remarkably the $EAS_n^{(6)}$-element with only six enhanced strain parameters is also free of locking. The pure displacement element Disp and the $EAS^{(9)}$-element are too stiff, as expected. The suggested

Table 5. Centerpoint deflection for undistorted mesh, $\nu = 0$

Element type	HR	Disp	$EAS_s^{(6)}$	$EAS_s^{(12)}$	$EAS^{(9)}$	$EAS^{(12)}$	$EAS^{(21)}$
w_c	0.97	0.0053	0.058	0.97	0.058	0.058	0.97

Table 6. Centerpoint deflection for undistorted mesh, $\nu = 0.3$

Element type	HR	Disp	$EAS_s^{(6)}$	$EAS_s^{(12)}$	$EAS^{(9)}$	$EAS^{(12)}$	$EAS^{(21)}$
w_c	0.888	0.0068	0.072	0.72	0.073	0.074	0.888

Table 7. Centerpoint deflection for undistorted mesh, $\nu = 0.499$

Element type	HR	Disp	$EAS_s^{(6)}$	$EAS_s^{(12)}$	$EAS^{(9)}$	$EAS^{(12)}$	$EAS^{(21)}$
w_c	0.74	0.0052	0.0077	0.0081	0.049	0.083	0.74

Table 8. Centerpoint deflection for distorted mesh, $\nu = 0.3$

Element type	HR	Disp	$EAS_s^{(6)}$	$EAS_s^{(12)}$	$EAS^{(9)}$	$EAS^{(12)}$	$EAS^{(21)}$
w_c (standard)	0.57	0.0064	0.065	0.51	0.066	0.066	0.58
w_c (modified)	0.57	0.0064	0.067	0.49	0.068	0.068	0.57

element modifications have no effect on the results for this example, as the element shapes are regular.

4.4. *Three-dimensional solid elements used in plate bending analysis*

A thin square plate with clamped edges with a side-length of 100, a thickness of 1.0 loaded by a center-load $P = 16.367$ is investigated to assess the performance of the different element formulations in plate bending. The main focus is on the capability of the elements to represent bending and shear action for distorted and undistorted element shapes. The plate is clamped along all edges and for symmetry reasons only one quarter is discretized with a $2 \times 2 \times 1$ mesh taking only one element in thickness direction. The elasticity modulus is chosen such that using the Kirchhoff theory a value of 1.0 for the centerpoint deflection is obtained as the analytical solution. The plate bending test is performed with Poisson ratios of 0.0, 0.3 and 0.499; results are listed in Tables 5–7.

The elements HR, $EAS^{(21)}$ and $EAS_s^{(12)}$ show an excellent bending behavior for this coarse *undistorted mesh*, however, the quality of the $EAS_s^{(12)}$-element decreases rapidly with increasing Poisson ratio, which could be expected. The other elements are handicapped by containing bilinear shear strains, which makes it impossible to model the plate correctly even in the case of $\nu = 0$. A clear shear-locking is observed for these elements.

In Table 8 the deflections for a *distorted mesh* are listed for $\nu = 0.3$. As expected, the performance of all elements decreases even for Hellinger–Reissner elements. The difference in the deflections between the HR, $EAS^{(21)}$, $EAS_s^{(12)}$ and the other elements is quite obvious. In the upper row the results for standard eight-point integrated elements with full static condensation are shown, whereas in the second row the deflections for the newly developed modified elements, which do not need numerical integration and only inversion of the individual diagonal blocks of the H-matrix (see Section 3.3) are listed. It is immediately visible that there is *no significant* difference between the elements formulated in standard fashion and their modified counterparts. This can be explained by the fact that the decreasing quality of the results are the effect of so-called thin mesh-locking (see Sze and Ghali, 1992), which occurs only in distorted meshes.

5. CONCLUSIONS

A family of trilinear three-dimensional solid elements based on Simo's enhanced strain formulation is presented and investigated. A systematic development of new reliable and efficient elements is given, for which neither numerical integration nor static condensation of the internal parameters is necessary. The enhanced strain interpolation terms are chosen to remove the locking tendencies from the displacement element. The numerical examples and comprehensive theoretical considerations indicate that the newly developed so-called modified elements satisfy the patch-test and yield satisfactory accuracy comparable to standard (= eight-point numerical integration and full static condensation) enhanced strain elements. Furthermore, for the set-up of the element-stiffness matrices or nodal-force vectors little numerical effort is needed. This is particularly remarkable for the elements with a large number of enhanced strain parameters. Thus these newly developed elements are perfectly suitable for large scale computations. Their corresponding counterparts for nonlinear analysis are currently under development.

Acknowledgements—The authors particularly acknowledge the inspiring work of Professor J. C. Simo, to whom this contribution is dedicated and who has been the driving force not only in the field covered by this paper, but for many other developments in computational structural mechanics. With his outstanding contributions he has set long lasting milestones.

REFERENCES

Andelfinger, U. and Ramm, E. (1993). EAS-elements for two-dimensional, three-dimensional, plate and shell structures and their equivalence to HR-elements. *Int. J. Numer. Meth. Engng* **36,** 1311–1337.

Beltyschko, T. and Bindeman, L. P. (1991). Assumed strain stabilization of the four-node quadrilateral with one-point quadrature for nonlinear problems. *Comput. Meth. Appl. Mech. Engng* **88,** 311–340.

Beltyschko, T. and Bindeman, L. P. (1993). Assumed strain stabilization of the eight-node hexahedral element. *Comput. Meth. Appl. Mech. Engng* **105,** 225–260.

Belytschko, T. and Wang, X. (1987). An efficient flexurally superconvergent hexahedral element. *Engng Comput.* **4,** 281–288.

Belytschko, T., Ong, J. S.-J., Liu, W. K. and Kennedy, J. M. (1984). Hourglass control in linear and nonlinear problems. *Comput. Meth. Appl. Mech. Engng* **54,** 279–301.

Flanagan, D. P. and Belytschko, T. (1981). A uniform strain hexahedron and quadrilateral with orthogonal hourglass control. *Int. J. Numer. Meth. Engng* **17,** 679–706.

Hughes, J. R. and Malkus, D. S. (1978). Mixed finite element methods—reduced and selective integration techniques: a unification of concepts. *Comput. Meth. Appl. Mech. Engng* **15,** 63–81.

Liu, W. K., Ong, J. S. and Uras, R. A. (1985). Finite element stabilization matrices—a unification approach. *Comput. Meth. Appl. Mech. Engng* **53,** 13–46.

Pian, T. H. and Sumihara, K. (1984). Rational approach for assumed stress finite elements. *Int. J. Numer. Meth. Engng* **20,** 1685–1695.

Simo, J. C. and Armero, F. (1992). Geometrically nonlinear enhanced-strain mixed methods and the method of incompatible modes. *Int. J. Numer. Meth. Engng* **33,** 1413–1449.

Simo, J. C., Armero, F. and Taylor, R. L. (1993). Improved versions of assumed enhanced strain tri-linear elements for three-dimensional finite deformation problems. *Comput. Meth. appl. Mech. Engng* **110,** 359–386.

Simo, J. C. and Rifai, M. S. (1990). A class of mixed assumed strain methods and the method of incompatible modes. *Int. J. Numer. Meth. Engng* **29,** 1595–1638.

Sze, K. Y. (1992). Efficient formulation of robust hybrid elements using orthogonal stress–strain interpolants and admissible matrix formulation. *Int. J. Numer. Meth. Engng* **35,** 1–20.

Sze, K. Y. and Ghali, A. (1992). A two-field solid element suiting thin-mesh analysis by admissible matrix formulation. *Engng Comput.* **9,** 649–668.

Taylor, R. L., Beresford, P. J. and Wilson, E. L. (1976). A non-conforming element for stress-analysis. *Int. J. Numer. Meth. Engng* **10,** 1211–1219.